DETERMINATION OF TURBULENT FLOW FIELD OVER A FLAT PLATE USING ENSEMBLE-AVERAGED NAVIER-STOKES EQUATIONS

by

S. P. Chandra Sekhar

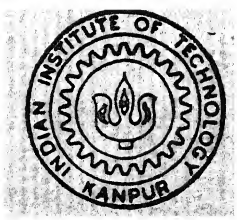

DEPARTMENT OF AEROSPACE ENGINEERING
INDIAN INSTITUTE OF TECHNOLOGY KANPUR
April 1994

DETERMINATION OF TURBULENT FLOW FIELD OVE
A FLAT PLATE USING ENSEMBLE-AVERAGED NAVIER-STOKES EQUATIONS

A thesis submitted
in partial fulfilment of the requirements
for the degree of

Master of Technology

by

S.P.Chandra Sekhar

to the

DEPARTMENT OF AEROSPACE ENGINEERING
INDIAN INSTITUTE OF TECHNOLOGY-KANPUR
April-1994

11.4.94

CERTIFICATE

It is certified that the work contained in the thesis entitled "DETERMINATION OF TURBULENT FLOW FIELD OVER A FLAT PLATE USING ENSEMBLE-AVERAGED NAVIER-STOKES EQUATIONS" by **S.P.Chandra Sekhar**, has been carried out under my supervision and that this work has not been submitted else where for a degree.

O P Sharma

Dr. O.P.Sharma
Professor
Dept. of Aerospace Engg.
Indian Institute of Technology
Kanpur

Date :6-4-1994
Place :I.I.T.,Kanpur

Dedicated to

my parents

Sri. S.P.Veera Bhadra Sastry

Smt. Swarajya Lakshmi

and to

my teacher

Dr. O.P.Sharma

Acknowledgement

First of all I wish to express my deep gratitude to Dr. O.P.Sharma for his valuable guidance and encouragement towards the successful completion of this work. I really enjoyed a great pleasure while working under him.

I am thankful to my friends V.Durga Prasad, N.Srinivas, U.V.Sarma G.Srinivas, M.Jaya Krishna, S.Arunkumar, Prashant Deb and Shamsi for their immemorable help at all stages of this work.

I am also thankful to my family members for their encouragement and moral support during my graduation.

At last, but not least, I wish to express my sincere thanks to the Computer Center and Central Library people for extending their cooperation.

Date : 6-4-1994
Place : I.I.T.Kanpur. S.P.C.S.

Abstract

The compressible, turbulent flow over a thin flat plate is analysed by solving ensemble-averaged Navier-Stokes equations. A computer code is developed based on time-dependent, multi-dimensional implicit finite difference scheme to solve the governing partial differential equations. The method due to Briley and McDonald involving time linearization and alternating-directional implicit technique is used. The discretization of the governing equations and the corresponding boundary conditions lead to a system of block tridiagonal form of algebraic equations containing the unknown flow variables at each grid point. Assuming uniform initial conditions and solving these algebraic equations result the solution of the flow field at the unknown time level. The process is repeated by marching in time direction until the solution attains steady state. A zero-equation Cebeci and Smith turbulence model is used to describe the turbulence of the flow. A second order artificial dissipation model is used at implicit time level to suppress the spatial oscillations developing due to central differencing of the convective terms and a fourth order explicit dissipation is used to smoothen the solution at each time step.

The flow field over the flat plate is analysed starting from the leading edge to the turbulent region. In the laminar region, the calculated velocity profile is compared with the known Blasius solution and a good agreement is found. Next, in the turbulent region, the calculated velocity is compared with Simpson's experimental data. For various input parameters, a comparison is made between the code prediction and an empirical correlation between the coefficient of local skin friction and local Reynolds no. along the plate length and a reasonably good agreement is found. Thus the general validity of the numerical scheme and computer code has been established.

Contents

List of Figures

NOTATIONS

x, y	Axes directions in Cartesian coordinate system
$\triangle x, \triangle y$	Grid spacing in x, y directions
η, ζ	Transformed coordinates for x and y
$\triangle \eta, \triangle \zeta$	Grid spacing in η, ζ directions
N_x	No. of grid points in x-direction
N_y	No. of grid points in y-direction
t	Time
$\triangle t$	Time step
ϕ	Flow variable
U	Velocity vector
u, v	Velocity components in x, y coordinate directions
ρ	Mass density
T	Temperature
p	Pressure
h	Enthalpy
c	Sonic velocity
μ	Molecular viscosity
k	Molecular conductivity
Re	Reynlods number
M	Mach number
Pr	Prandtl number
C_f	Coefficient of local skin friction $= \frac{\tau_w}{1/2\rho_\infty u_\infty^2}$
$\frac{D}{Dt}$	Total derivative

C_p, C_v	Specific heats at constant pressure and volume
γ	Ratio of specific heats
R	Gas constant
∇	Vector operator
Φ	Viscous dissipation term
q	Heat flux vector
γ_{tr}	Intermittency factor
l	Mixing length
A	Damping constant
C, A^+, κ	constants in turbulence model
Π	Strength of wake
Ψ_ϕ	$\phi - \phi^n$
$\tau_{i,j}$	Shear stress tensor
$e_{i,j}$	Strain tensor
$\delta_{i,j}$	Kroneckor delta
σ_d	Parameter in artificial viscosity
δ	Displacement thickness
θ	Momentum thickness
σ_x, σ_y	Transformation parameters
CFL	Courant Friedrichs and Lewy number
H, D, S	Functions of ϕ in the conservative form
ADI	Alternating Directional Implicit technique
pde	Partial Differential Equation

subscripts

t	Turbulent quantity
eff	Effective quantity
art	Artificial quantity
r	Characteristic quantity
x_{tr}	x at transition
∞	Free stream condition

superscripts

n	Known time level
$n+1$	Unknown time level
$*$	Intermediate time level
$\tilde{}$	Physical quantity
$-$	Ensemble averaged quantity
$'$	Fluctuation

Chapter 1

Introduction

1.1 General

Most of the flows encountered in nature and engineering systems are turbulent. These are highly unsteady with random fluctuations in both space and time. It presents some of the most difficult problems both in fundamental understanding of its behaviour as well as in obtaining solutions of realistic situations, many of which are still unresolved. An important characteristic of turbulence is the richness of scales associated with eddy motion present in the flow. The flow over an aircraft wing, cascade flows, rocket motor internal flows are some examples of real life turbulent flows.

In fluids of low viscosity, the steady laminar flow tends to become unstable at high Reynolds numbers. This instability due to small disturbances is an initial step in the process whereby a laminar flow undergoes transition and then becomes fully turbulent. The description of transition again, is a big difficulty due to lack of understanding of the underlying phenomena.

The flow field can be analysed either by conducting an experiment or calculating theoretically. These two methods have their own advantages and disadvantages. Though the experiments will give the most realistic answers for many flow situations, however, the cost, sensitivity, accuracy etc. of the equipment and measuring instruments are the limiting factors. Moreover, in performing experiments it is not always possible to simulate the true operating conditions of the prototype. Furthermore, there is also a need of refinement of

the existing measuring techniques for real complex flows.

On the other hand, in theoretical approach, the flow field physics is translated into mathematical equations resulting, in general, in a set of differential equations. These generally reflect conservation of mass, momentum, and energy of the fluid, which when solved with appropriate boundary conditions give the solution of the flow field. Unlike the laboratory experiments, this approach does not entail any problems such as probe size limitations, etc. and information can be obtained about quantities which are difficult or impossible to measure in the laboratory such as the instantaneous pressure in the interior of the flow, hot flow fields etc.. The general solution can be obtained in some simple cases by analytical methods, however, in many cases of practical interest, analytical solutions are not possible due to the complex forms of the governing differential equations. These types of problems can be handled conveniently to some extent by numerical methods using a high speed digital computer.

The development of equations governing the fluid motion started with Navier in 1822 and the subsequent contributions by St.Venant, Poisson and Stokes led to the present day well known Navier-Stokes equations. These are a set of nonlinear mixed type coupled partial differential equations, and are considered to be the corner stones of the Continuum Newtonian Fluid Dynamics. These conservation equations are valid for the turbulent flows as well, however, the values of the flow variables are to be replaced by their instantaneous values since it is a fluctuating flow [8].

One approach to deal with the existence of turbulence is to solve the equations for a set of boundary conditions and initial values for a large number of instants of time and then to compute the mean values (known as the ensemble-averaged solutions). But this is a hopeless undertaking even for a most restricted problem such as the case of incompressible flow, because it requires large amount of computation as well as computer memory, which is beyond the capacity of the present day computers. In view of these limitations, in another way, the solution of the turbulent flow makes use of statistical averaging procedures to average the governing equations and then solving these mean flow equations rather than averaging over the solutions. The averaging can be either time averaging, mass-weighted averaging or ensemble-averaging [8]. This averaging of the equations give rise to new terms and require some approximations to close the system of equations. These additional terms are related with mean flow variables through turbulence models and can be interpreted as

apparent stress gradients and heat flux quantities associated with the turbulent fluctuating quantities.

Different models have been developed with different levels of approximations to close the set of mean equations. The models can be generally classified into Eddy Viscosity models and Reynolds Stress models [16]. There are various eddy viscosity models of varying sophistication. The simplest model is due to Boussinesq (1877) in which the turbulent stresses in the mean momentum equations are expressed as the product of a turbulent viscosity and the mean velocity tensor gradient. The turbulent viscosity also called eddy viscosity is proportional to the mean velocity. Further development involves the well known Prandtl mixing length concept (1925) in which the eddy viscosity is expressed in terms of the mean velocity gradient. This turbulent viscosity is a property of the flow whereas the molecular viscosity is the property of the fluid and this concept of eddy viscosity is phenomenological and has no mathematical basis. The eddy viscosity can be prescribed algebraically in terms of the quantities such as turbulent kinetic energy and dissipation which are obtained by solving the corresponding partial differential equations. Depending on the type and number of equations employed for turbulent quantities, these are called algebraic or zero equation, one equation and two equation models. Zero-equation models are based on mixing length and eddy viscosity concepts and are being widely used in practical engineering applications. The turbulent kinetic energy pde, associated with the so-called *velocity scale*, in case of one-equation model and in case of two-equation model along with the turbulent kinetic energy pde, the turbulent dissipation pde, associated with the so-called *length scale*, are added to the governing equations through the mean variables to determine the turbulent viscosity. The one and two-equation models are employed when additional details on turbulence quantities are needed [16].

The other models are Reynolds stress model, algebraic Reynolds stress model and large eddy simulation. Reynolds stress model employs several pde's for components of the turbulence stress tensor. This is one of the most complex models in the current literature. The Reynolds stress model is under extensive development and is employed in complex flow situations, three-dimensional flows, flows with curvature, rotation, blowing or suction etc. In algebraic Reynolds stress models, approximations are made to reduce the governing pde's of the Reynolds stresses to algebraic equations. These equations are coupled to transport equations of the two-equation models to find the turbulence and flow field. In large eddy simulation the time dependent, three-dimensional, large eddy structure

is resolved through a numerical solution of the time dependent Navier-Stokes equations and a low level model for the small scale turbulence is employed. This kind of simulation is prohibitively expensive and it's use is presently limited to very simple flows. With slight variations in different empirical constants of these various models are reported, suitable to specific types of problems. But there is no universal model applicable to all types of flows so far .

To reduce the complexity of the problem, different levels of approximations are made to the original Navier-Stokes equations such as boundary layer equations, parabolized Navier-Stokes equations, etc. [1]. In parabolized equations, also called thin layer Navier-Stokes equations, the mean momentum equation in normal direction is considered but the stream wise momentum diffusion is neglected. In boundary layer equations the normal direction mean momentum equations are also neglected. These kinds of simplifications are found to be reasonable only in certain situations. The need to solve the full equations is still remained for a variety of real life situations like flow at a corner, the flow over a launch vehicle, etc..

The unsteady compressible Navier-Stokes equations are, in general, a mixed set of hyperbolic and parabolic type equations whereas the unsteady incompressible Navier-Stokes equations are a mixed set of elliptic and parabolic type equations. If the unsteady terms are dropped from compressible equations, the resulting equations become a mixed set of hyperbolic and elliptic type equations. These are difficult to solve because of the different numerical techniques required for each of them. As a consequence, nearly all successful solutions of the compressible Navier-Stokes equations have employed the unsteady form of equations. The steady state of solution is obtained by marching the solution in time until prescribed accuracy in convergence is achieved. Explicit, implicit and weighted average of explicit and implicit techniques are the basic methods to solve these time dependent equations.

In explicit methods, the spatial gradients are evaluated using known conditions at the old time level. These methods are simpler, easy to code, and vectorizable. The implementation of the boundary conditions is also easy. But the major disadvantage is the requirement to satisfy the stability condition as dictated by the CFL criterion and thereby large number of time marching steps are needed. In the implicit methods, the spatial derivatives are evaluated at the unknown time level. This permits the use of higher time

steps, so faster convergence can be achieved. But for each time step, solution is obtained by solving a set of algebraic equations which needs again a big computation.In the implicit methods, due to the large time steps, there will be more truncation error, and results relatively inaccurate transient path. So this method is a most attractive if the steady state solution is only important rather than the transient solutions. The weighted average of explicit and implicit method uses the earlier two concepts with some weightages. For example, the Crank-Nicolson method, in which equal weightage is used.

Direct solutions in these methods involve inversion of a block pentadiagonal matrix for 2D problems, and block septadiagonal matrix for 3D problems at each time level, which consume large CPU time, so approximate factorization is often employed to convert this into a simple block tridiagonal system. This in turn introduces a factorization error and may lead to stability problems. So some care should be taken regarding the time step while developing the solution. Some of the earlier methods utilized the explicit techniques, while later development involved the implicit schemes.

For solving the fluid dynamics equations, there are various numerical methods as summarized below:

1. Finite Difference Method (FDM) : In this method a mesh is superimposed over the flow field, with the mesh lines along the coordinate directions. The derivatives in the pdes are replaced by their finite difference approximations and the unknown variables will be evaluated at each grid point by solving the resultant system of algebraic equations [1].

2. Finite Volume Method (FVM) : In this method the computational domain is divided into a network of finite volumes. The equations of fluid dynamics are used in integral form. The unknown vector and fluxes are staggered, i.e., the unknown vector is required at centroids of finite volumes, while the fluxes are required at the surfaces of these volumes. The network of the volumes can be arbitrary and numerical quadrature is used to replace flux integrals in terms of values of the unknowns at the centroids [1].

3. Finite Element Method (FEM) : The domain is divided into several finite elements which can be triangles, tetrahedrons quadrilaterals or hexahedral elements etc. A piece-wise linear approximation to the unknowns in terms of their values at the nodes

of the finite elements is assumed. Minimization of the error gives the solution at the nodal [14].

4. Particle In Cell Method (PIC) : A mesh is required in this method also. The transport terms are simulated by movement of particles from cell to cell. The pressure gradient and viscous terms are treated by finite differencing. The PIC method is thus a combination of Lagrangian and Eulerian description of fluid flow. Further development of this model is Statistical PIC Method. In this method stochastic model equivalent to the PDE is used for numerical simulation. This approach is also called Monte-Carlo Method [19].

5. Spectral Methods (SM) : The unknown is expressed in terms of basis functions like Chebychev polynomials or trigonometric functions over a mesh. The amplitudes of various modes can be obtained from the data at the mesh points. The space derivatives can be then obtained by differentiating the Fourier expansion. Then the PDE is reduced to a set of ODE by taking its inner product with basis functions. The resultant ODE can be solved by differencing the time derivatives [7].

6. Cellular Automata or Lattice Gas Dynamics (CA) : The computational domain is divided into a fine mesh called lattice. At the lattice points particles are located having velocities with directions along the mesh lines passing through the lattice points. The transport term is simulated by shifting the particles to neighbouring lattice points. A collision cycle of calculations is then performed during which pre-collisions velocities of particles are replaced by post collision velocities [10].

Out of these methods FDM, FVM, FEM are well developed while the remaining methods are presently in developing stage. For a simple geometry, with uniform grids, Finite Difference Methods are suitable. These are simple, easy to understand, having relatively less algorithm complexity, and recommended by many researchers also.

Several computer codes have been reported in the literature to solve different levels of approximated equations during the past decade or so. Some of them are MINT developed by McDonald and his associates, ARC-2D and ARC-3D developed by Pulliam and Steger, TEACH developed by Spalding group, NISA/3D Fluid developed by EMRC. Troy, USA etc. Few of them are made available on commercial basis also. Relevant journal articles appear in AIAA Journal, Computers and Fluids, Computer Methods in Applied

Mechanics and Engineering, Journal of Computational Physics, Journal of Fluid Mechanics, Numerical Heat Transfer, Transactions of ASME., Journal of Fluids Engineering, and some of the important books in this area are given in the list of references.

1.2 Present Investigation

As mentioned earlier there are different forms of approximated Navier-Stokes equations which are applicable in particular situations only. In the cases of mixing of the viscid and inviscid flows, chemically reacting flows or flows having complicated geometries such as flow at slots, submerged nozzles of rocket motor etc, the approximated equations will not represent the entire physics of the problem and in such situations the simplified equations are not valid. Therefore, there exists a need to solve the full equations for the entire domain.

In the present investigation, for simplicity, the flow over a thin flat plate is considered. Adjacent to the plate there will be a boundary layer and it will be laminar and then gradually undergoes transition and becomes fully turbulent as the flow moves from the leading edge to trailing edge of the plate. The coefficient of wall friction, the thickness of the boundary layer and other flow variables vary along the plate length. Getting a detailed steady solution for a turbulent flow field over a thin flat plate by solving the ensemble-averaged Navier-Stokes equations is the goal of the present investigation.

The steady state solution is obtained by marching in time direction until the convergence in time is reached . A mesh, clustered , near the wall is superimposed over the flow field and an implicit finite difference method is used to solve the governing conservation equations. Briley and McDonald [5] developed a split linearised block implicit numerical scheme to solve the multi-dimensional unsteady Navier-Stokes equations using alternating direction implicit technique and tested it for a laminar flow in the entrance region of a duct. Further, Sabnis et al. [21] used it to solve the solid propellent rocket motor internal flows. The same procedure is adopted here to solve the external turbulent flow over a flat plate. This method is a one-step method, as opposed to a predictor-corrector method, and requires no iterations to compute the solution at single time step. Cebeci and Smith turbulence model [8] is used for the turbulent viscosity in turbulent boundary layer. Further a second order artificial dissipation model and a fourth order smoothing terms are

included to suppress the spatial wiggles. A computer code is developed to solve this flow field and validated with the available data.

The details of the method of solution , the results and conclusions are described in the following chapters.

Chapter 2

Problem Formulation

2.1 The Flow Field Description

The flow over a thin flat plate is analysed by solving the general Navier-Stokes equations for a turbulent flow. A schematic diagram of the flow field is shown in Figure 2.1. It is considered that the fluid is a viscous, compressible, chemically non-reacting, perfect gas with zero bulk viscosity coefficient, constant molecular viscosity, thermal conductivity and specific heats. The flow over the plate is considered with zero pressure gradient. The plate is very thin with smooth surface and is fixed so that the flow field oscillations due to turbulence are not transmitted to it. Thermodynamically, the plate is assumed as perfectly adiabatic and no heat transfer takes place. Alternate conditions for wall thermal conditions and for pressure gradient can also be incorporated.

Adjacent to the plate, there will be viscous and thermal boundary layers. Near the leading edge, the flow in the boundary layer is laminar and it becomes unstable as it moves in downstream. Then the flow undergoes transition in which the disturbances grow, and these disturbances increase in the flow and becomes fully turbulent as it moves further downstream (see Figure 2.1). The flow in the turbulent layer is more dissipative in nature, and no longer be similar. The boundary layer thickness, the velocity gradients at wall surface, etc. vary along the length of the plate. There will be heating of the fluid also due to the viscous effects as it moves downstream.

The fluid motion at any instant of time is described by the well-known Navier-

Stokes equations, which are the statements of conservation of mass, momentum, and energy of the fluid. In order to deal with turbulent flow, as mentioned earlier, the mean flow equations can be obtained by using ensemble-averaging. The ensemble-average of a variable is defined as the arithmetic mean measured over the many identical experiments [17].

Denoting the ensemble average of a fluctuating variable $u(t)$ as $\overline{u(t)}$, it is defined as

$$\overline{u(t)} = \lim_{N\to\infty} \frac{1}{N} \sum_{j=1}^{N} [\, u(t) \,]_j \tag{2.1}$$

Similarly, the ensemble average of a function $g(u)$, say, $\overline{g(u)}$ is defined as

$$\overline{g(u)} = \lim_{N\to\infty} \frac{1}{N} \sum_{j=1}^{N} [\, g\,[u(t)] \,]_j \tag{2.2}$$

An instantaneous variable, say, u can be represented as a sum of a mean quantity $\overline{u}$ and a fluctuating quantity u'. Thus

$$u = \overline{u} + u' \tag{2.3}$$

In the process of averaging the following rules have been used for averaging different quantities.

$$\overline{\overline{u}u'} = \overline{u}\,\overline{u'} = 0 \tag{2.4}$$

$$\begin{aligned} \overline{u_i\, u_j} &= \overline{(\,\overline{u_i} + u_i'\,)\,(\,\overline{u_j} + u_j'\,)} \\ &= \overline{u_i}\,\overline{u_i} + \overline{u_i'\, u_j'} \end{aligned} \tag{2.5}$$

and so on. The application of this averaging procedure to the governing differential equations give rise to the mean equations. The resulting mean equations, thus contain some additional terms in view of the turbulent fluctuations and are modelled by introducing the concept of turbulent viscosity and conductivity as described in the previous chapter.

2.2 Governing Equations

The governing equations of a turbulent flow field over a thin adiabatic flat plate, such as the ensemble-averaged Navier-Stokes equations, describing the conservation of mass, momentum, and energy of the fluid along with the equation of state for perfect gas are

given below in vector form [22]. The variables in the following equations are ensemble averaged physical quantities, and for simplicity the symbols *overbar* and *tilde* are removed.

Continuity equation :

$$\frac{\partial \rho}{\partial t} + \nabla \cdot (\rho U) = 0 \tag{2.6}$$

Momentum Conservation equation :

$$\frac{\partial}{\partial t} (\rho U) + \nabla \cdot (\rho U U) = - \nabla p + \nabla \cdot \tau \tag{2.7}$$

Where

τ is the stress tensor (both molecular and turbulent) given by

$$\tau_{ij} = 2 \mu_{eff} e_{ij} - \frac{2}{3} \mu_{eff} \nabla \cdot U \delta_{ij} \tag{2.8}$$

e_{ij} is the rate of strain tensor, given by

$$e_{ij} = \frac{1}{2} \left(\frac{\partial U_i}{\partial x_j} + \frac{\partial U_j}{\partial x_i} \right) \tag{2.9}$$

μ_{eff} is the effective viscosity and is the sum of the molecular and turbulent viscosities. That is,

$$\mu_{eff} = \mu + \mu_t \tag{2.10}$$

The turbulent viscosity is obtained from the turbulence model and will be described later.

Energy conservation equation :

$$\frac{\partial}{\partial t} (\rho h) + \nabla \cdot (\rho U h) = \frac{Dp}{Dt} - \nabla \cdot q + \Phi \tag{2.11}$$

Where

Φ is the viscous dissipation per unit volume, is given by

$$\Phi = \mu_{eff} \left[2 e_{ij} e_{ij} - \frac{2}{3} (\nabla \cdot U)^2 \right] \tag{2.12}$$

q is the heat flux vector, is given by

$$q = - k_{eff} \nabla T \tag{2.13}$$

k_{eff} is the effective conductivity and is the sum of the molecular and turbulent conductivities. That is,

$$k_{eff} = k + k_t \tag{2.14}$$

The turbulent conductivity is obtained from the turbulence model.

Equation of state for perfect gas :

$$p = \rho R T \tag{2.15}$$

The pressure term in the above equations can be eliminated by using the equation of state for perfect gas. The energy equation Eq.(2.11), can be rewritten in terms of temperature as follows.

$$C_v \left[\frac{\partial}{\partial t} (\rho T) + \nabla \cdot (\rho U T) \right] = - \nabla \cdot q + \Phi - \rho R T \nabla \cdot U \tag{2.16}$$

These governing equations are coupled, nonlinear and mixed type partial differential equations. The momentum equation written in vector form Eq.(2.7) leads to two momentum equations in each x and y directions. There are four pdes such as Eqs.(2.5), (2.7) and (2.16) and an equation of state for perfect gas Eq.(2.15) and five unknown variables such as ρ, U (consisting of u and v), T and p and these can be solved with proper boundary conditions as described below.

2.3 Boundary Conditions

The following boundary conditions can be obtained by studying the flow field over the flat plate. The above set of equations are solved subjected to these boundary conditions.

Along the plate surface no slip conditions hold good and the plate is assumed as adiabatic, thus

Along the wall: at $y = 0$:

$$u = v = 0 \tag{2.17}$$

$$\frac{\partial T}{\partial y} = 0 \tag{2.18}$$

The density at wall is calculated from the simplified form of the continuity equation at wall surface.

$$\frac{\partial \rho}{\partial t} + \frac{\partial}{\partial y}(\rho v) = 0 \tag{2.19}$$

Pressure gradient along the dominant flow direction is taken as zero. This gives the boundary conditions at the free stream boundary that the density, velocity, temperature are constant and equal to free stream values. As this boundary is taken at sufficiently far from the plate surface, the gradients of the density, velocity, temperature in normal to plate at this boundary are set to zero. Thus

Along the free stream boundary : as $y \longrightarrow \infty$:

$$u = u_\infty ; \quad v = 0 ; \quad T = T_\infty ; \quad \rho = \rho_\infty \tag{2.20}$$

$$\frac{\partial \rho}{\partial y} = \frac{\partial u}{\partial y} = \frac{\partial v}{\partial y} = \frac{\partial T}{\partial y} = 0 \tag{2.21}$$

At the upstream boundary the flow is entering uniformly at zero angle of attack. This condition leads to

Along the upstream boundary : at $x = 0$:

$$u = u_\infty ; \quad v = 0 ; \quad T = T_\infty ; \quad \rho = \rho_\infty \tag{2.22}$$

At the downstream end of the plate, there is lack of information regarding the flow, it is, therefore, necessary to model the boundary conditions at this end. This is done by setting the second derivatives of the velocity components, temperature in x direction are zero. The boundary conditions for density is modelled through equation of state for perfect gas. Thus

Along the down stream boundary : at $x = L$:

$$\frac{\partial^2 u}{\partial x^2} = \frac{\partial^2 v}{\partial x^2} = \frac{\partial^2 T}{\partial x^2} = 0 \tag{2.23}$$

For the initial conditions, uniform flow is assumed in the entire domain, and the velocity components at the wall are set to zero.

2.4 Non-Dimensionalization

The governing fluid dynamic equations are very often put in the non-dimensional form as it leads to some advantages. For instance, that the flow variables can be *normalised* so that their values will fall in between certain prescribed limits such as *0* and *1*. Also the characteristic parameters of the flow field can be obtained such as Mach number (M), Reynolds number (Re), Prandtl number (Pr) which can be varied independently. A generalized way of non-dimensionalization is used as described below.

For non-dimensionalization, the various characteristic parameters are taken as follows. The plate length (L) is taken as characteristic length (L_r), the free stream density, velocity, temperature, molecular viscosity, molecular conductivity (ρ_∞, u_∞, T_∞, μ_∞, k_∞ are taken as corresponding characteristic quantities (ρ_r, u_r, T_r, μ_r, k_r) and for time, the convective time (L_∞/u_∞) is taken as characteristic time (t_r). And the non-dimensionalization procedure is as follows.

$$x = \frac{\tilde{x}}{L_r}; \quad y = \frac{\tilde{y}}{L_r}; \quad \rho = \frac{\tilde{\rho}}{\rho_r} \tag{2.24}$$

$$u = \frac{\tilde{u}}{u_r}; \quad v = \frac{\tilde{v}}{u_r}; \quad T = \frac{\tilde{T}}{T_r} \tag{2.25}$$

$$p = \frac{\tilde{p}}{\rho_r u_r^2}; \quad h = \frac{\tilde{h}}{\rho_r u_r^2}; \quad t = \frac{\tilde{t}}{L_r/u_r} \tag{2.26}$$

$$\mu = \frac{\tilde{\mu}}{\mu_r}; \quad k = \frac{\tilde{k}}{k_r} \tag{2.27}$$

Corresponding to these non-dimensional expressions, different first and second order derivatives are expressed and substituting these in the governing equations Eqs.(2.6 to 2.16), various non-dimensional parameters are obtained such as :

$$\text{Mach number} = M = \frac{u_r}{c} \tag{2.28}$$

$$\text{Reynolds number} = Re = \frac{\rho_r \, u_r \, L_r}{\mu_r} \tag{2.29}$$

$$\text{Prandtl number} = Pr = \frac{\mu_r \, C_p}{k_r} \tag{2.30}$$

After non-dimensionalization the governing conservation equations are rewritten in a matrix form as follows.

$$\frac{\partial H(\phi)}{\partial t} = D(\phi) + S(\phi) \tag{2.31}$$

Where ϕ is a column vector, H and S are column vector functions of ϕ and D is a column vector whose elements are spatial differential operators. The various elements of these matrices are given below.

$$H(\phi) = \left(\rho,\ \rho u,\ \rho v,\ \rho T \right)^{\tau} \tag{2.32}$$

$$D_x(\phi) = \begin{pmatrix} -\dfrac{\partial}{\partial x}(\rho u) \\ -\dfrac{\partial}{\partial x}\left(\rho u^2 + \dfrac{1}{\gamma M^2}\rho T\right) + \dfrac{\mu_{eff}}{Re}\dfrac{\partial^2 u}{\partial x^2} + \dfrac{4}{3\,Re}\dfrac{\partial \mu_{eff}}{\partial x}\dfrac{\partial u}{\partial x} \\ -\dfrac{\partial}{\partial x}(\rho u v) + \dfrac{\mu_{eff}}{Re}\dfrac{\partial^2 v}{\partial x^2} - \dfrac{2}{3\,Re}\dfrac{\partial \mu_{eff}}{\partial y}\dfrac{\partial u}{\partial x} \\ -\dfrac{\partial}{\partial x}(\rho u T) + (1-\gamma)\rho T\dfrac{\partial u}{\partial x} \\ +\dfrac{\gamma\, k_{eff}}{Re\,Pr}\dfrac{\partial^2 T}{\partial x^2} + \dfrac{\gamma}{Re\,Pr}\dfrac{\partial T}{\partial x}\dfrac{\partial k_{eff}}{\partial x} \end{pmatrix} \tag{2.33}$$

$$D_y(\phi) = \begin{pmatrix} -\dfrac{\partial}{\partial y}(\rho v) \\ -\dfrac{\partial}{\partial y}(\rho u v) + \dfrac{\mu_{eff}}{Re}\dfrac{\partial^2 u}{\partial y^2} - \dfrac{2}{3\,Re}\dfrac{\partial \mu_{eff}}{\partial x}\dfrac{\partial v}{\partial y} \\ -\dfrac{\partial}{\partial y}\left(\rho v^2 + \dfrac{1}{\gamma M^2}\rho T\right) + \dfrac{\mu_{eff}}{Re}\dfrac{\partial^2 v}{\partial y^2} + \dfrac{4}{3\,Re}\dfrac{\partial \mu_{eff}}{\partial y}\dfrac{\partial v}{\partial y} \\ -\dfrac{\partial}{\partial x}(\rho v T) + (1-\gamma)\rho T\dfrac{\partial v}{\partial y} \\ +\dfrac{\gamma\, k_{eff}}{Re\,Pr}\dfrac{\partial^2 T}{\partial y^2} + \dfrac{\gamma}{Re\,Pr}\dfrac{\partial T}{\partial y}\dfrac{\partial k_{eff}}{\partial y} \end{pmatrix} \tag{2.34}$$

$$S(\phi) = \begin{pmatrix} 0 \\ \frac{\mu_{eff}}{3\,Re}\frac{\partial}{\partial x}(\nabla\cdot U) + \frac{\partial \mu_{eff}}{\partial y}\left(\frac{\partial u}{\partial y} + \frac{\partial v}{\partial x}\right) \\ \frac{\mu_{eff}}{3\,Re}\frac{\partial}{\partial y}(\nabla\cdot U) + \frac{\partial \mu_{eff}}{\partial x}\left(\frac{\partial u}{\partial y} + \frac{\partial v}{\partial x}\right) \\ \gamma(\gamma - 1)\,M^2\,\frac{\mu_{eff}}{Re}\,[\Phi] \end{pmatrix} \tag{2.35}$$

2.5 Non-Dimensional Boundary Conditions

The following non-dimensional boundary conditions are obtained by normalising the boundary conditions given in Section 2.3.

At $y = 0$:

$$u = v = 0 \tag{2.36}$$

$$\frac{\partial T}{\partial y} = 0 \tag{2.37}$$

The density at wall is calculated by simplifying the continuity equation at wall as follows

$$\frac{\partial \rho}{\partial t} + \frac{\partial}{\partial y}(\rho\, v) = 0 \tag{2.38}$$

As $y \longrightarrow \infty$:

$$u = 1;\quad v = 0;\quad T = 1;\quad \rho = 1 \tag{2.39}$$

$$\frac{\partial \rho}{\partial y} = \frac{\partial u}{\partial y} = \frac{\partial v}{\partial y} = \frac{\partial T}{\partial y} = 0 \tag{2.40}$$

At $x = 0$:

$$u = 1;\quad v = 0;\quad T = 1;\quad \rho = 1 \tag{2.41}$$

At $x = L$:

$$\frac{\partial^2 u}{\partial x^2} = \frac{\partial^2 v}{\partial x^2} = \frac{\partial^2 T}{\partial x^2} = 0 \tag{2.42}$$

Similarly, the initial conditions in the entire domain become unity, and the velocity components at the wall are become zero.

2.6 Turbulence Modelling

In order to close the system of mean flow equations, the turbulent stresses and turbulent heat flux vectors have to be modelled through the mean flow variables. Therefore, following the laminar flow description, the turbulent stress is expressed as a product of a turbulent viscosity and mean flow velocity gradient and the turbulent heat flux as a product of turbulent conductivity and temperature gradient. As mentioned earlier different models have been developed to describe the turbulent viscosity with different level of empiricism. Here the so-called *Zero-equation* model developed by Cebeci and Smith [8] is adopted.

This model is based on the eddy viscosity and mixing length concepts. The turbulent boundary layer is regarded as a composite layer of a thin laminar sub-layer, an inner layer and an outer layer. The thin laminar sub-layer is neglected in the present model. The inner region is much smaller than the outer region, with thickness about 10 to 20 % of the total boundary layer thickness. In the inner region, turbulent viscosity is expressed algebraically in terms of the mean velocity gradient and a mixing length . The mixing length is expressed in terms of distance from the wall as earlier proposed by VanDriest (1956) [15] and subsequently extended by including a damped law of wall. In the outer region, turbulent viscosity is described in terms of the velocity defect as proposed by Coles [8].

In most practical calculations, it is necessary to deal with the laminar, transient and turbulent domains of the boundary layer. According to Emmon's spot theory (1951) [13], the flow in the transition region is intermittently turbulent. The transition region can be accounted by considering the expression for intermittency factor given by Chen and Thyson [9]. This expression is based on Dhawan and Narasimha's intermittency expression (1958)[11] for incompressible flows.

The various expressions of the Zero-equation model due to Cebeci and Smith are given below.

In the inner region : $0 \leq y \leq y_c$:

$$\mu_t = \rho\, l^2 \left| \frac{\partial u}{\partial y} \right| \gamma_{tr} \tag{2.43}$$

$$\text{where} \quad l = \kappa\, y\, [\, 1 - exp(\, -y/A\,)\,] \tag{2.44}$$

In the outer region : $y_c \leq y \leq \delta$:

$$\mu_t = \rho\,\alpha \left| \int_0^\infty (u_\infty - u)\, dy \right| \gamma_{tr} \tag{2.45}$$

y_c is determined from the continuity of the eddy viscosity across the boundary layer. The inner region expression is applied outwards from the wall until the two expressions give the same value of the turbulent viscosity (μ_t) The variables appearing in the above equations are as follows.

A is damping constant given by

$$A = A^+ \frac{\mu}{\rho N} \left(\frac{\tau_w}{\rho_w} \right)^{\frac{1}{2}} \left(\frac{\rho}{\rho_w} \right)^{\frac{1}{2}} \tag{2.46}$$

$$A^+ = 26 \tag{2.47}$$

$$\kappa = 0.41 \tag{2.48}$$

For flows with no mass transfer :

$$N = \left[1 - 11.8 \left(\frac{\mu_w}{\mu_\infty} \right) \left(\frac{\rho_\infty}{\rho_w} \right)^2 p^+ \right]^{\frac{1}{2}} \tag{2.49}$$

For flows with mass transfer :

$$N = \left[\frac{\mu}{\mu_\infty} \left(\frac{\rho_\infty}{\rho_w} \right)^2 \frac{p^+}{v_w^+} \left[1 - exp\left(11.8\, v_w^+ \frac{\mu_w}{\mu} \right) \right] + exp\left(11.8\, v_w^+ \frac{\mu_w}{\mu} \right) \right]^{\frac{1}{2}} \tag{2.50}$$

where

$$p^+ = - \frac{\mu\, u_\infty}{\rho\, u_\tau^3} \frac{\partial u_\infty}{\partial x} \tag{2.51}$$

$$u_\tau = \left(\frac{\tau_w}{\rho} \right)^{1/2} \tag{2.52}$$

$$v_w^+ = \frac{v_w}{u_\tau} \tag{2.53}$$

For values of $R_\theta < 5000$:

$$\alpha = 0.0168 \frac{1.55}{1 + \Pi} \tag{2.54}$$

Π = strength of the wake

$$= 0.55 \left[1 - exp\left(- 0.243\, z_1^{1/2} - 0.298\, z_1 \right) \right] \tag{2.55}$$

$$z_1 = \left(\frac{R_\theta}{425} - 1 \right) \tag{2.56}$$

For values of $R_\theta \geq 5000$:

$$\alpha = 0.0168 \tag{2.57}$$

The intermittencey factor, γ_{tr} accounts for the transition region. For two dimensional flows, it is defined as

$$\gamma_{tr} = 1 - exp\left[-G\,(x - x_{tr})\left(\int_{x_{tr}}^{x} \frac{1}{u_\infty}\,dx\right)\right] \tag{2.58}$$

x_{tr} is the x location where the transition begins. G is an empirical factor given by

$$G = \frac{3}{C^2}\frac{u_\infty^3}{\nu^2}\,Re_{x_{tr}}^{1.34} \tag{2.59}$$

$$Re_{x_{tr}} = \frac{\rho_\infty\, u_\infty\, x_{tr}}{\mu_\infty} \tag{2.60}$$

$$C = 60 + 4.86M^{1.92} \tag{2.61}$$

For $0 < M < 5$

For a two dimensional flows, the transition Reynolds number can be estimated from the following empirical expression given by Cebeci and Smith [8].

$$Re_{\theta_{tr}} = 1.174\left[1 + \left(\frac{22400}{Re_{x_{tr}}}\right)\right] Re_{x_{tr}}^{0.46} \tag{2.62}$$

A constant turbulent Prandtl number equal to 0.92 is assumed (for air) and is used to calculate the turbulent conductivity. The expression for turbulent Prandtl number is given below.

$$Pr_t = \frac{\mu_t\, C_p}{k_t} = 0.92 \tag{2.63}$$

Here the turbulent kinetic energy is not used in the turbulent viscosity formulation, it implies that the mean motion is uneffected by turbulence intensity and the length scale.

This model can be used in two dimensional flows with mild pressure gradients and mild curvature with no flow separation or rotation effects. It is useful in computing three dimensional boundary layers with small cross flows and mild pressure gradients having no curvature or rotation effects. Lakshminarayana [16] concluded that for an attached two dimensional boundary layer with a mild pressure gradient, there is very little advantage in restoring to a higher order models. The algebraic model is adequate for the prediction of the mean velocity field. However, for flow with strong adverse pressure gradient (close to separation) and flows with strong favorable pressure gradient (laminarizing), this formulation is only adequate but not sufficient.

2.7 Artificial Dissipation

The steady flow over a flat plate is generally a high Reynolds number flow except in the region near the leading edge. Central differencing of the first derivatives in the Navier-Stokes equations equations leads to spatial oscillations and further the solution diverges also some times at these high Reynolds numbers. To suppress these spatial oscillations, excess viscosity is provided, while developing the solution, through artificial dissipation models. This artificial dissipation can be provided either by adding the artificial viscosity terms explicitly to the governing equations or one side discretization of the convective terms such as upwinding or hybrid schemes [19]. Various models of adding artificial dissipation for high Reynolds flows have been investigated by Shamroth et al.[23] and evaluated in the context of a one dimensional model problem.

In the present application, a term of a form

$$\frac{\partial}{\partial x}\left(\mu_{art}\,\frac{\partial \phi}{\partial x}\right) \tag{2.64}$$

s added in the unknown time level to the governing equations [21]. This explicit dissipa-ion is added in the dominant flow direction only (that is in x-direction), but not in the ıormal direction (y-direction), so that the boundary layer effects will not be affected. The ariable ϕ denotes the velocity component u for x-direction momentum equation, velocity omponent v for y-direction momentum equation, density ρ for continuity equation and he enthalpy h for energy equation.

The coefficient μ_{art} is obtained from an expression given by

$$\rho\, u\, \triangle x \quad \leq \quad \left(\frac{1}{\sigma_d}\right)\,[\,\overline{\mu}\,+\,\mu_{art}\,] \tag{2.65}$$

where

$$\triangle x \quad = \quad \text{grid spacing at the point in question} \tag{2.66}$$

$$\overline{\mu} \quad = \quad 0 \qquad \text{for continuity equation} \tag{2.67}$$

$$= \quad \mu_{eff} \qquad \text{for momentum equations} \tag{2.68}$$

$$= \quad \frac{\mu_{eff}}{Pr} \qquad \text{for energy equation} \tag{2.69}$$

ıe parameter σ_d initially taken as 0.5, which corresponds to the well-known concept of ell-Reynolds number of 2. After obtaining a converged solution with $\sigma_d = 0.5$, its value

is reduced to 0.05 and further to 0.005, and the solution procedure further marches in time to obtain the final converged solution.

In order to suppress the high frequency oscillations in the solution a fourth order explicit dissipation term is added at known time level to the right hand side of the governing equations as follows.

$$- \epsilon_e \left[(\triangle y)^4 \frac{\partial^4(\phi)}{\partial y^4} \right] \tag{2.70}$$

This fourth order term does not effect the formal accuracy of the algorithm. The $-$ ve sign to the above fourth order derivative is required in order to produce positive damping. The smoothing coefficient ϵ_e should be less than approximately $1/16$ for stability [2], presently 0.05 is used.

2.8 Non-Uniform Grid Stretching

Local refinement of mesh where there will be large gradients is always advisable to predict them more accurately. In the present problem, the velocity components, temperature, and density vary largely near the wall. So it is better to have a small grid spacing near the wall and large grid spacing in the outer region rather than uniform small grid spacing in the entire domain. But discretization of the governing equations with variable grid spacing is a difficult procedure. This variable grid spacing can be handled conveniently by transforming the coordinates (x, y) to another set of coordinates (η, ζ) with uniform grid spacing. An analytical coordinate transformation devised by Robert's [20] is adopted here for a non uniform grid generation and is described below.

If N_y grid points are to be used in the range of $0 < y < 1$ and if steep gradients are to be expected in a region of thickness of σ near $y = 0$, then Roberts transformation $\zeta(y)$ is given by

$$\zeta(\, y\,) \quad = \quad N_y \, + \, (\, N_y \, - \, 1\,) \log\left(\frac{y \, + \, a \, - \, 1}{y \, + \, a \, + \, 1} \right) / \log\left(\frac{a \, - \, 1}{a \, + \, 1} \right) \tag{2.71}$$

$$\text{where} \quad a^2 \; = \; 1/(\, 1 \, - \, \sigma\,) \tag{2.72}$$

Then the corresponding partial derivatives are as follows.

$$\frac{\partial}{\partial y} \quad = \quad \frac{\partial \zeta}{\partial y} \frac{\partial}{\partial \zeta} \tag{2.73}$$

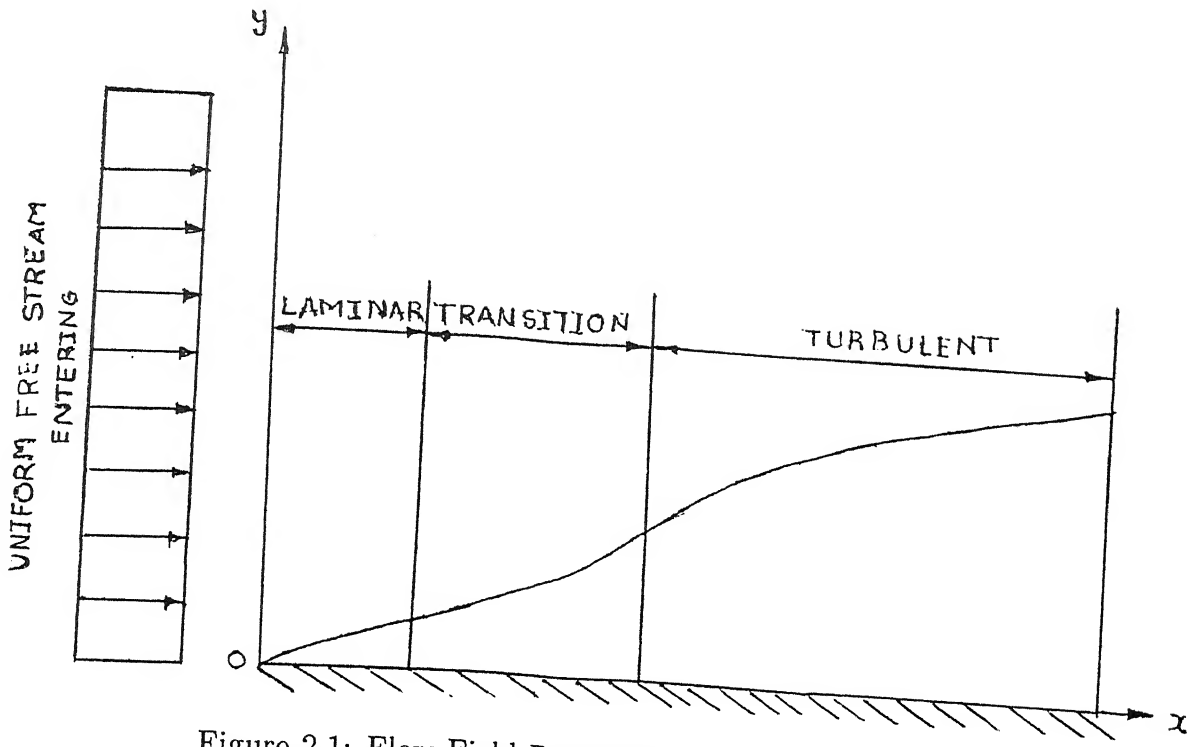

Figure 2.1: Flow Field Description on a Thin Flat Plate

$$\frac{\partial^2}{\partial y^2} = \left(\frac{\partial^2 \zeta}{\partial y^2}\right)\frac{\partial}{\partial \zeta} + \left(\frac{\partial \zeta}{\partial y}\right)^2 \frac{\partial^2}{\partial \zeta^2} \tag{2.74}$$

$$\frac{\partial \zeta}{\partial y} = f(\zeta)$$

$$= \frac{(N_y - 1)}{\log\left(\frac{a+1}{a-1}\right)} \frac{\left(1 - e^{A1}\right)^2}{2e^{A1}} \tag{2.75}$$

$$\frac{\partial^2 \zeta}{\partial y^2} = f(\zeta)$$

$$= \frac{(N_y - 1)}{4 \log\left(\frac{a+1}{a-1}\right)} \left(b^2 - b^{-2} - 2b + 2b^{-1}\right) \tag{2.76}$$

$$\text{where} \quad b = \left(\frac{a+1}{a-1}\right)^{\left(\frac{\zeta - N_y}{N_y - 1}\right)} \tag{2.77}$$

The transformation in x-direction is optional, according to the lengths of laminar, transition and turbulent boundary layers and the requirements of solution in different zones. The same transformation can be used in x-direction also. The (x, y) plane corresponding to a plane of uniform grid spacing (η, ζ) plane and the dependency of grid stretching on N_y and σ are shown in Figure 2.2 and 2.3.

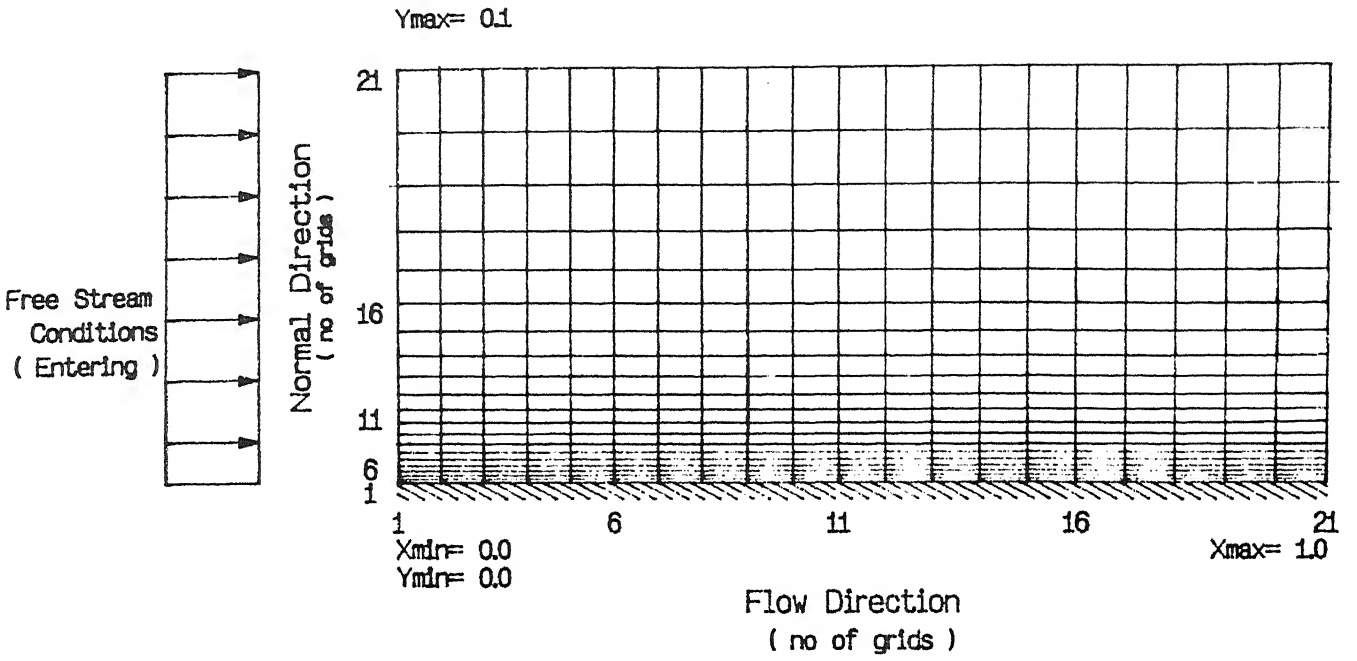

Figure 2.2: Non-Uniform Mesh. For $N_x = N_y = 21$. $\sigma_x = 0.99$, $\sigma_y = 0.01$.

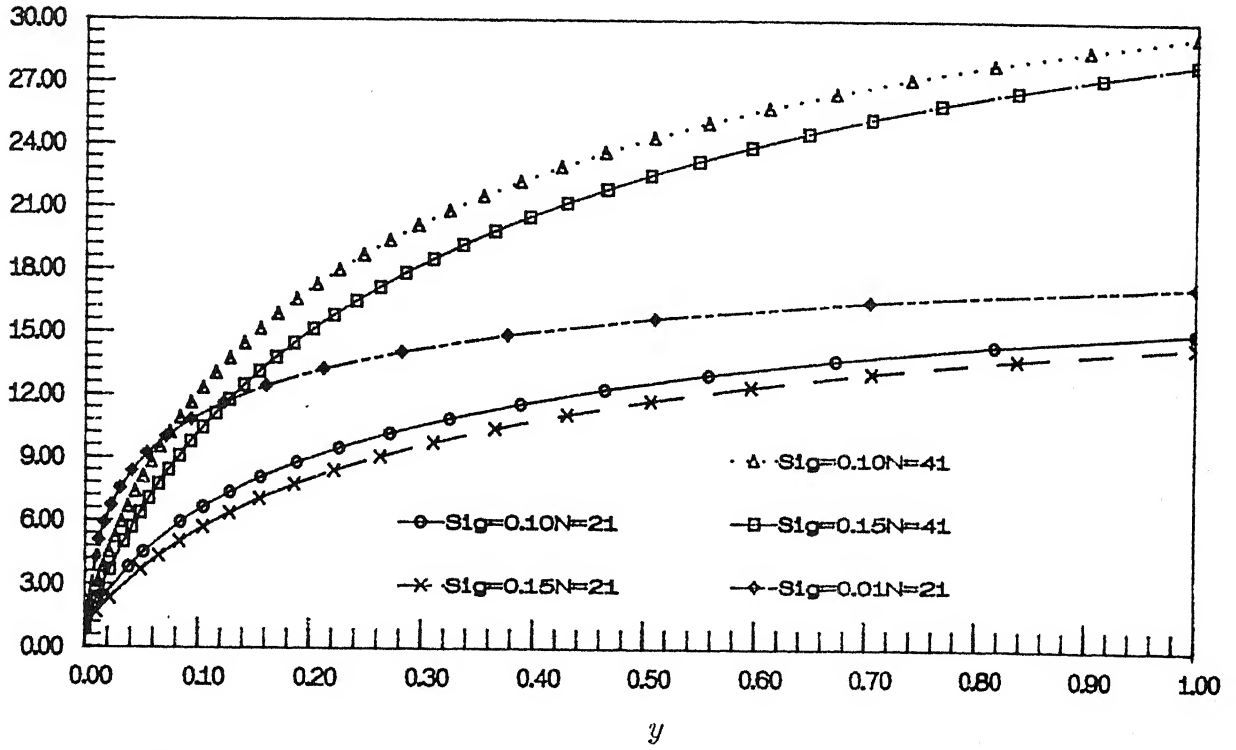

Figure 2.3: Dependency of Grid Points Cluster on Various Parameters

Chapter 3

Method Of Solution

3.1 General Outline

The governing equations of a turbulent flow over a thin flat plate and the corresponding boundary conditions along with the required turbulence modelling and artificial dissipation have been described in the previous chapter. An alternating-directional implicit finite difference method is used to solve these set of coupled partial differential equations numerically.

In the governing equations, the time derivatives are replaced by a forward time difference approximation. The terms involving the non-linearities at the implicit time level are linearized by expanding them about the known time solution by using Taylor's expansion. The spatial derivatives are replaced by the central difference approximations at implicit time level, for both first and second order derivatives. An alternating-directional implicit scheme is used to reduce the complexity of the computing the solution. This converts the two dimensional problem into a set of one dimensional problems corresponding to each line of grid points of the mesh.

This leads to a system of coupled linear difference equations having a tridiagonal block-banded structure. By solving these block-banded equations the unknown variables at $n+1$ time level can be obtained.

Initially, turbulence viscosity is set equal to zero for a few time marching steps. The turbulence viscosity is then calculated from the turbulence model as discussed earlier

by using the mean flow solution over the flow field at the known time level. This turbulent viscosity is used for solution at the unknown time level. Thus the marching process is repeated until the solution attains the steady state. As the solution approaches asymptotically to the steady state, the marching procedure is stopped when the consecutive solution's difference falls within the specific minimum value, in the present analysis, this is taken as 0.000001.

The various steps involved in the solution procedure are discussed in detail in the following sections.

3.2 Time-Linearization

In order to linearize the non-linear terms appearing in the implicit time governing equations, various linearizing techniques are available in the literature. Out of them the method of extrapolating the coefficients, is adopted here. This method is having certain advantages, but it makes the equations complicated. This procedure requires no iterations to update the coefficients at any time level so that the computational cost will be reduced comparatively. It may be pointed out that rather than utilizing the computation time, as in other linearizing methods, to iterate only for the sake of reducing the truncation error associated with linearization, the overall accuracy might be improved in the present method by using the same computation time to reduce the marching time step size.

The technique is based on Taylor's expansion of non-linear implicit terms about the solution at the known time level t^n. This leads to a one step, two level scheme, which is being linear in unknown quantities and can be solved efficiently with out any iteration. Formally the truncation error of this procedure can be made as small as required. Here, in view of computational cost, first order approximation is considered, which neglects the second and higher order terms in Taylor's expansion [1]. The procedure of linearization is explained below.

Considering the Eq.(2.31) at implicit time level

$$\frac{\partial H(\phi)^{n+1}}{\partial t} = D(\phi)^{n+1} + S(\phi)^{n+1} \tag{3.1}$$

Replacing with implicit time difference approximations,

$$\left(\frac{H(\phi)^{n+1} - H(\phi)^n}{\Delta t} \right) = D(\phi)^{n+1} + S(\phi)^{n+1} \tag{3.2}$$

The various quantities are expanded as follows.

$$H(\phi)^{n+1} = H(\phi)^n + \left(\frac{\partial H(\phi)}{\partial \phi} \right)^n \left(\frac{\partial \phi}{\partial t} \right) \Delta t + O(\Delta t)^2 \tag{3.3}$$

$$D(\phi)^{n+1} = D(\phi)^n + \left(\frac{\partial D(\phi)}{\partial \phi} \right)^n \left(\frac{\partial \phi}{\partial t} \right) \Delta t + O(\Delta t)^2 \tag{3.4}$$

$$S(\phi)^{n+1} = S(\phi)^n + \left(\frac{\partial S(\phi)}{\partial \phi} \right)^n \left(\frac{\partial \phi}{\partial t} \right) \Delta t + O(\Delta t)^2 \tag{3.5}$$

The term $\left(\frac{\partial \phi}{\partial t} \right) \Delta t$ is approximated further by $(\phi^{n+1} - \phi^n)$. Thus the Eq.(3.2) becomes a linear implicit time difference form as follows.

$$\frac{\partial H(\phi)^n}{\partial \phi} \left(\frac{\phi^{n+1} - \phi^n}{\Delta t} \right) = D(\phi)^n + S(\phi)^n + \left(\frac{\partial D(\phi)^n}{\partial \phi} + \frac{\partial S(\phi)^n}{\partial \phi} \right) \left(\frac{\phi^{n+1} - \phi^n}{\Delta t} \right) \tag{3.6}$$

On examination, it can be seen that Eq.(3.6) is linear in the quantity $(\phi^{n+1} - \phi^n)$. Computationally, it is convenient to solve the Eq.(3.6) for $(\phi^{n+1} - \phi^n)$ rather than ϕ^{n+1}. This also simplifies the roundoff errors. So introducing a new variable Ψ such that

$$\Psi = \phi - \phi^n \tag{3.7}$$

$$\text{so that} \quad \Psi^{n+1} = \phi^{n+1} - \phi^n \tag{3.8}$$

$$\text{and} \quad \Psi^n = 0 \tag{3.9}$$

Rewriting the Eq.(3.6) in a convenient way

$$(A + \Delta t\, B)\, \Psi^{n+1} = \Delta t \, [D(\phi)^n + S(\phi)^n] \tag{3.10}$$

$$\text{where} \quad A = \frac{\partial H(\phi)^n}{\partial \phi} - \Delta t \left(\frac{\partial S(\phi)^n}{\partial \phi} \right) \tag{3.11}$$

$$B = - \frac{\partial D(\phi)^n}{\partial \phi} \tag{3.12}$$

Applying the above linearization procedure to each of the conservation equations the following forms are obtained.

Continuity Equation :

The continuity equation in implicit time difference form, is

$$\left(\frac{\rho^{n+1} - \rho^n}{\triangle t} \right) + \frac{\partial}{\partial x} (\rho u)^{n+1} + \frac{\partial}{\partial y} (\rho v)^{n+1} = 0 \tag{3.13}$$

Expanding the nonlinear quantities by Taylor's expansion as explained before

$$\begin{aligned} (\rho u)^{n+1} &= (\rho u)^n + \left[\frac{\partial}{\partial \rho} (\rho u) \frac{\partial \rho}{\partial t} + \frac{\partial}{\partial u} (\rho u) \frac{\partial u}{\partial t} \right]^n \triangle t + O (\triangle t)^2 \\ &= (\rho u)^n + \left[u^n \left(\frac{\rho^{n+1} - \rho^n}{\triangle t} \right) + \rho^n \left(\frac{u^{n+1} - u^n}{\triangle t} \right) \right] \triangle t + O (\triangle t)^2 \\ &= (\rho u)^n + u^n \Psi_\rho^{n+1} + \rho^n \Psi_u^{n+1} \end{aligned} \tag{3.14}$$

Similarly,

$$(\rho v)^{n+1} = (\rho v)^n + v^n \Psi_\rho^{n+1} + \rho^n \Psi_v^{n+1} \tag{3.15}$$

substituting the above expressions in Eq.(3.13), the continuity equation becomes

$$\begin{aligned} & \Psi_\rho^{n+1} + \triangle t \frac{\partial}{\partial x} \left(u^n \Psi_\rho^{n+1} + \rho^n \Psi_u^{n+1} \right) + \triangle t \frac{\partial}{\partial y} \left(v^n \Psi_\rho^{n+1} + \rho^n \Psi_v^{n+1} \right) \\ = & - \triangle t \left[\frac{\partial}{\partial x} (\rho u)^n + \frac{\partial}{\partial y} (\rho v)^n \right] \end{aligned} \tag{3.16}$$

x-momentum equation :

The x-momentum equation is written in an implicit time difference form. For the sake of convenience, the cross derivatives in the viscous dissipation term are treated at explicit time level, (that is at known time level). This makes the splitting of equations for alternating direction is easier.

$$\begin{aligned} & \frac{(\rho u)^{n+1} - (\rho u)^n}{\triangle t} + \frac{\partial}{\partial x} \left(\rho u^2 \right)^{n+1} + \frac{\partial}{\partial y} (\rho u v)^{n+1} \\ = & - \frac{\partial p^{n+1}}{\partial x} + \frac{\mu_{eff}}{Re} \left[\left(\frac{\partial^2 u^{n+1}}{\partial x^2} + \frac{\partial^2 u^{n+1}}{\partial y^2} \right) + \frac{1}{3} \frac{\partial}{\partial x} \left(\frac{\partial u^n}{\partial x} + \frac{\partial v^n}{\partial y} \right) \right] \\ & + \frac{1}{Re} \left[\frac{\partial \mu_{eff}}{\partial x} \left(\frac{4}{3} \frac{\partial u^{n+1}}{\partial x} - \frac{2}{3} \frac{\partial v^{n+1}}{\partial y} \right) + \frac{\partial \mu_{eff}}{\partial y} \left(\frac{\partial u^n}{\partial y} + \frac{\partial v^n}{\partial x} \right) \right] \end{aligned} \tag{3.17}$$

The various nonlinear terms are expressed as follows

$$\left(\rho u^2 \right)^{n+1} = (\rho u)^n + (u^2)^n \Psi_\rho^{n+1} + (2 \rho u)^n \Psi_u^{n+1} \tag{3.18}$$

$$(\rho u v)^{n+1} = (\rho u v)^n + (\rho u)^n \Psi_v^{n+1} + (\rho v)^n \Psi_u^{n+1} + (u v)^n \Psi_\rho^{n+1} \tag{3.19}$$

and like wise for other terms. Further, the term pressure p is replaced by $\rho T/\gamma M^2$, by using the equation of state for perfect gas. The x-momentum equation in the linearised implicit form becomes

$$\begin{aligned}
&\left[u^n \Psi_\rho^{n+1} + \rho^n \Psi_u^{n+1} \right] + \Delta t \left[\frac{\partial}{\partial x} \left(\left(u^2 \right)^n \Psi_\rho^{n+1} + 2 \left(\rho u \right)^n \Psi_u^{n+1} \right) \right] \\
+ \quad & \Delta t \left[\frac{\partial}{\partial y} \left(\left(uv \right)^n \Psi_\rho^{n+1} + \left(\rho u \right)^n \Psi_v^{n+1} + \left(\rho v \right)^n \Psi_u^{n+1} \right) \right] \\
+ \quad & \frac{\Delta t}{\gamma M^2} \left[\frac{\partial}{\partial x} \left(\rho^n \Psi_T^{n+1} + T^n \Psi_\rho^{n+1} \right) \right] - \frac{\Delta t \, \mu_{eff}}{Re} \left[\frac{\partial^2 \Psi_u^{n+1}}{\partial x^2} + \frac{\partial^2 \Psi_u^{n+1}}{\partial y^2} \right] \\
- \quad & \frac{\Delta t}{Re} \left[\frac{\partial \mu_{eff}}{\partial x} \left(\frac{4}{3} \frac{\partial \Psi_u^{n+1}}{\partial x} - \frac{2}{3} \frac{\partial \Psi_v^{n+1}}{\partial y} \right) \right] \\
= \quad & - \Delta t \left[\frac{\partial}{\partial x} \left(\rho u^2 \right)^n + \frac{1}{\gamma M^2} \frac{\partial \rho T^n}{\partial x} + \frac{\partial \rho u v^n}{\partial y} \right] \\
& + \frac{\Delta t \, \mu_{eff}}{Re} \left[\frac{\partial^2 u^n}{\partial x^2} + \frac{\partial^2 u^n}{\partial y^2} \right] + \frac{\Delta t \, \mu_{eff}}{3 \, Re} \left[\frac{\partial^2 u^n}{\partial x^2} + \frac{\partial^2 v^n}{\partial x \partial y} \right] \\
& + \frac{\Delta t}{Re} \left[\frac{\partial \mu_{eff}}{\partial x} \left(\frac{4}{3} \frac{\partial u^n}{\partial x} - \frac{2}{3} \frac{\partial v^n}{\partial y} \right) + \frac{\partial \mu_{eff}}{\partial y} \left(\frac{\partial u^n}{\partial y} + \frac{\partial v^n}{\partial x} \right) \right] \qquad (3.20)
\end{aligned}$$

y-momentum equation :

Similarly, the y-momentum equation is written in implicit time difference form, again the cross derivatives are written at old time level.

$$\begin{aligned}
&\frac{\left(\rho v \right)^{n+1} - \left(\rho v \right)^n}{\Delta t} + \frac{\partial}{\partial x} \left(\rho uv \right)^{n+1} + \frac{\partial}{\partial y} \left(\rho v^2 \right)^{n+1} \\
= \quad & - \frac{\partial p^{n+1}}{\partial y} + \frac{\mu_{eff}}{Re} \left[\left(\frac{\partial^2 v^{n+1}}{\partial x^2} + \frac{\partial^2 v^{n+1}}{\partial y^2} \right) + \frac{1}{3} \frac{\partial}{\partial y} \left(\frac{\partial u^n}{\partial x} + \frac{\partial v^n}{\partial y} \right) \right] \\
& + \frac{1}{Re} \left[\frac{\partial \mu_{eff}}{\partial x} \left(\frac{\partial u^n}{\partial y} + \frac{\partial v^n}{\partial x} \right) + \frac{\partial \mu_{eff}}{\partial y} \left(\frac{4}{3} \frac{\partial v^{n+1}}{\partial y} - \frac{2}{3} \frac{\partial u^{n+1}}{\partial x} \right) \right] \qquad (3.21)
\end{aligned}$$

Writing in the linearised form, after expanding the non-linear terms according to Taylor's expansion as described before and replacing the pressure term p by $\rho T/\gamma M^2$

$$\begin{aligned}
&\left[v^n \Psi_\rho^{n+1} + \rho^n \Psi_v^{n+1} \right] \\
+ \quad & \Delta t \left[\frac{\partial}{\partial x} \left(\left(\rho u \right)^n \Psi_v^{n+1} + \left(\rho v \right)^n \Psi_u^{n+1} + \left(uv \right)^n \Psi_\rho^{n+1} \right) \right] \\
+ \quad & \Delta t \left[\frac{\partial}{\partial y} \left(\left(v^2 \right)^n \Psi_\rho^{n+1} + 2 \left(\rho u \right)^n \Psi_v^{n+1} \right) \right] + \frac{\Delta t}{\gamma M^2} \left[\frac{\partial}{\partial y} \left(\rho^n \Psi_T^{n+1} + T^n \Psi_\rho^{n+1} \right) \right]
\end{aligned}$$

$$
\begin{aligned}
- \quad & \frac{\triangle t\ \mu_{eff}}{Re}\left[\frac{\partial^2\Psi_u^{n+1}}{\partial y^2}+\frac{\partial^2\Psi_v^{n+1}}{\partial y^2}\right]-\frac{\triangle t}{Re}\left[\frac{\partial\mu_{eff}}{\partial x}\left(\frac{4}{3}\frac{\partial\Psi_v^{n+1}}{\partial y}-\frac{2}{3}\frac{\partial\Psi_u^{n+1}}{\partial x}\right)\right] \\
= \quad & -\triangle t\left[\frac{\partial}{\partial x}(\rho uv)^n+\frac{\partial}{\partial y}\left(\rho v^2\right)^n+\frac{1}{\gamma M^2}\frac{\partial}{\partial y}(\rho T)^n\right] \\
& +\frac{\triangle t\ \mu_{eff}}{Re}\left[\frac{\partial^2 v^n}{\partial x^2}+\frac{\partial^2 v^n}{\partial y^2}\right]+\frac{\triangle t\ \mu_{eff}}{3\ Re}\left[\frac{\partial^2 u^n}{\partial y\partial x}+\frac{\partial^2 v^n}{\partial y^2}\right] \\
& +\frac{\triangle t}{Re}\left[\frac{\partial\mu_{eff}}{\partial x}\left(\frac{\partial u^n}{\partial y}+\frac{\partial v^n}{\partial x}\right)+\frac{\partial\mu_{eff}}{\partial y}\left(\frac{4}{3}\frac{\partial u^n}{\partial x}-\frac{2}{3}\frac{\partial v^n}{\partial y}\right)\right] \qquad (3.22)
\end{aligned}
$$

Energy equation :

The energy equation in the implicit time difference form is given below. To reduce the complexity, the dissipation term Φ is treated explicitly, though it can be discretised at implicit level.

$$
\begin{aligned}
& \frac{(\rho T)^{n+1}-(\rho T)^n}{\triangle t}+\frac{\partial}{\partial x}(\rho uT)^{n+1}+\frac{\partial}{\partial y}(\rho vT)^{n+1} \\
= \quad & \frac{\gamma\ k_{eff}}{Re\ Pr}\left[\frac{\partial^2 T^n}{\partial x^2}+\frac{\partial^2 T^n}{\partial y^2}\right]-\gamma(\gamma-1)\ M^2\ p^{n+1}\left[\frac{\partial u^{n+1}}{\partial x}+\frac{\partial v^{n+1}}{\partial y}\right] \\
& +\gamma(\gamma-1)\ M^2\ \frac{\mu_{eff}}{Re}[\Phi]+\frac{\gamma}{Re\ Pr}\left[\frac{\partial T}{\partial x}\frac{\partial k_{eff}}{\partial x}+\frac{\partial T}{\partial y}\frac{\partial k_{eff}}{\partial y}\right] \qquad (3.23)
\end{aligned}
$$

Where Φ is the dissipation function, defined earlier in Eq.(2.12). The pressure term p is replaced by $\rho T/\gamma M^2$,as before. Writing the energy equation in the linearised form, after expanding the non-linear terms according to Taylor's expansion as described earlier,

$$
\begin{aligned}
& \left[T^n\Psi_\rho^{n+1}+\rho^n\Psi_T^{n+1}\right] \\
+ \quad & \triangle t\left[\frac{\partial}{\partial x}\left((\rho u)^n\Psi_T^{n+1}+(\rho T)^n\Psi_u^{n+1}+(uT)^n\Psi_\rho^{n+1}\right)\right] \\
+ \quad & \triangle t\left[\frac{\partial}{\partial y}\left((\rho v)^n\Psi_T^{n+1}+(\rho T)^n\Psi_v^{n+1}+(vT)^n\Psi_\rho^{n+1}\right)\right] \\
+ \quad & \triangle t\ (\gamma-1)\left[\left(T\frac{\partial u}{\partial x}\right)^n\Psi_\rho^{n+1}+\left(\rho\frac{\partial u}{\partial x}\right)^n\Psi_T^{n+1}+(\rho T)^n\frac{\partial\Psi_u^{n+1}}{\partial x}\right] \\
+ \quad & \triangle t\ (\gamma-1)\left[\left(T\frac{\partial v}{\partial x}\right)^n\Psi_\rho^{n+1}+\left(\rho\frac{\partial v}{\partial x}\right)^n\Psi_T^{n+1}+(\rho T)^n\frac{\partial\Psi_v^{n+1}}{\partial x}\right] \\
- \quad & \frac{\triangle t\ \gamma\ k_{eff}}{Re\ Pr}\left[\frac{\partial^2\Psi_T^{n+1}}{\partial x^2}+\frac{\partial^2\Psi_T^{n+1}}{\partial y^2}\right] \\
- \quad & \frac{\triangle t\ \gamma}{Re\ Pr}\left[\frac{\partial k_{eff}}{\partial x}\frac{\partial\Psi_T^{n+1}}{\partial x}+\frac{\partial k_{eff}}{\partial y}\frac{\partial\Psi_T^{n+1}}{\partial y}\right]
\end{aligned}
$$

$$= - \Delta t \left[\frac{\partial}{\partial x} (\rho u T)^n + \frac{\partial}{\partial y} (\rho v T)^n \right] + \frac{\Delta t \ \gamma \ k_{eff}}{Re \ Pr} \left[\frac{\partial^2 T^n}{\partial x^2} + \frac{\partial^2 T^n}{\partial y^2} \right]$$
$$+ \frac{\Delta t \ \gamma \ (\gamma - 1) \ M^2}{Re} [\Phi]^n - \gamma \ (\gamma - 1) \ (\rho T)^n \left[\frac{\partial u^n}{\partial x} + \frac{\partial v^n}{\partial y} \right]$$
$$+ \frac{\Delta t \ \gamma}{Re \ Pr} \left[\frac{\partial T^n}{\partial x} \frac{\partial k_{eff}}{\partial x} + \frac{\partial T^n}{\partial y} \frac{\partial k_{eff}}{\partial y} \right] \qquad (3.24)$$

3.3 Alternating-Directional Implicit Technique

Direct solving of the all coupled equations in the entire domain needs inversion of a penta-diagonal block banded matrix (for 2-D problems). This needs large memory as well as large computation. These can be reduced by applying an alternating-direction implicit technique, which results an easily solvable narrow (tridiagonal) block banded matrix. An alternating-direction implicit technique, developed by Douglas and Gunn [12] is adopted here.

The operator D in Eq.(2.31) is assumed that it contains only the derivatives of first and second order with respect to$x$ and y, but no mixed derivatives. This D operator can be split into two operators, D_x and D_y associated with the x and y coordinate directions and each having a functional form

$$D_x = F \left(\phi, \frac{\partial}{\partial x}, \frac{\partial^2}{\partial x^2} \right) \qquad (3.25)$$

$$D_y = F \left(\phi, \frac{\partial}{\partial y}, \frac{\partial^2}{\partial y^2} \right) \qquad (3.26)$$

Then the Eq.(3.10) becomes

$$[A + \Delta t \ (B_x + B_y)] \ \Psi^{n+1} = \Delta t \ [(D_x + D_y) \phi^n + S^n] \qquad (3.27)$$

The Douglus and Gunn representation of the above equations can be written as a two step solution procedure as follows.

First ADI step :

$$[A + \Delta t \ (B_x)] \ \Psi^* = \Delta t \ [(D_x + D_y) \phi^n + S^n] \qquad (3.28)$$

Second ADI step :

$$[A + \Delta t \ (B_y)] \ \Psi^{n+1} = A \ \Psi^* \qquad (3.29)$$

where Ψ^* is an intermediate solution.

The major attraction of this method is that the intermediate solution is a consistent approximation. Furthermore, the steady solution when $\Psi^n = \Psi^* = \Psi^{n+1} = 0$; is independent of Δt . Thus, physical boundary conditions for Ψ^{n+1} can be used in the intermediate steps without a serious loss in accuracy, with no loss for steady solution [5]. In this respect the Douglas and Gunn scheme appears to have an advantage over locally one-dimensional (LOD) or *splitting* schemes in which the intermediate steps do not satisfy the consistency condition [2]. As pointed out by Douglas and Gunn [12] the mixed derivatives can also be treated implicitly within the ADI framework, but this would increase the number of intermediate steps and thereby complicate the solution procedure.

The above alternating-directional implicit technique is applied to the conservative equations. Then the equations are transformed into a new set of coordinates (η, ζ) as discussed in section 2.8. Discretizing the spatial derivatives according to the three point central difference approximations for both second and first order derivatives, the following equations are obtained.

Continuity equation :
After first ADI step

$$\begin{aligned}
& \Psi^*_{\rho\, i-1}\left[-\frac{\Delta t}{2\,\Delta\eta}\left(\frac{\partial\eta}{\partial x}\right)_i u^n_{i-1}\right] + \Psi^*_{\rho\, i} + \Psi^*_{\rho\, i+1}\left[\frac{\Delta t}{2\,\Delta\eta}\left(\frac{\partial\eta}{\partial x}\right)_i u^n_{i+1}\right] \\
+ \quad & \Psi^*_{u\, i-1}\left[-\frac{\Delta t}{2\,\Delta\eta}\left(\frac{\partial\eta}{\partial x}\right)_i \rho^n_{i-1}\right] + \Psi^*_{u\, i+1}\left[\frac{\Delta t}{2\,\Delta\eta}\left(\frac{\partial\eta}{\partial x}\right)_i \rho^n_{i+1}\right] \\
= \quad & -\frac{\Delta t}{2\,\Delta\eta}\left(\frac{\partial\eta}{\partial x}\right)_i \left[\rho^n_{i+1}\, u^n_{i+1} - \rho^n_{i-1}\, u^n_{i-1}\right] \\
& + \frac{\Delta t}{2\,\Delta\zeta}\left(\frac{\partial\zeta}{\partial y}\right)_j \left[\rho^n_{j+1}\, u^n_{j+1} - \rho^n_{j-1}\, u^n_{j-1}\right]
\end{aligned} \tag{3.30}$$

After second ADI step

$$\begin{aligned}
& \Psi^{n+1}_{\rho\, j-1}\left[-\frac{\Delta t}{2\,\Delta\zeta}\left(\frac{\partial\zeta}{\partial y}\right)_j v^n_{j-1}\right] + \Psi^{n+1}_{\rho\, j} + \Psi^{n+1}_{\rho\, j+1}\left[\frac{\Delta t}{2\,\Delta\zeta}\left(\frac{\partial\zeta}{\partial y}\right)_j v^n_{j+1}\right] \\
+ \quad & \Psi^{n+1}_{u\, j-1}\left[-\frac{\Delta t}{2\,\Delta\zeta}\left(\frac{\partial\zeta}{\partial y}\right)_j \rho^n_{j-1}\right] + \Psi^{n+1}_{u\, j+1}\left[\frac{\Delta t}{2\,\Delta\zeta}\left(\frac{\partial\zeta}{\partial y}\right)_j \rho^n_{j+1}\right] \\
= \quad & \Psi^*_{\rho\, j}
\end{aligned} \tag{3.31}$$

x-momentum equation :

After first ADI step

$$
\begin{aligned}
& \Psi^{*}_{\rho\, i-1}\left[-\frac{\triangle t}{2\,\triangle\eta}\left(\frac{\partial\eta}{\partial x}\right)_i (u^2_{i-1})^n - \frac{\triangle t}{2\,\triangle\eta}\left(\frac{\partial\eta}{\partial x}\right)_i \frac{1}{\gamma\, M^2}\, T^n_{i-1}\right] + \Psi^{*}_{\rho\, i}\,[\,u^n_i\,] \\
+ \quad & \Psi^{*}_{\rho\, i+1}\left[-\frac{\triangle t}{2\,\triangle\eta}\left(\frac{\partial\eta}{\partial x}\right)_i \left(u^2_{i+1}\right)^n + \frac{\triangle t}{2\,\triangle\eta}\left(\frac{\partial\eta}{\partial x}\right)_i \frac{1}{\gamma\, M^2}\, T^n_{i+1}\right] \\
+ \quad & \Psi^{*}_{u\, i-1}\left[-2\,\frac{\triangle t}{2\,\triangle\eta}\left(\frac{\partial\eta}{\partial x}\right)_i \rho^n_{i-1}\, u^n_{i-1}\right. \\
& \qquad \left. + \frac{\triangle t}{2\,\triangle\eta}\,\frac{\mu_{eff}}{Re}\left(\frac{\partial^2\eta}{\partial x^2}\right)_i - \frac{\triangle t}{(\triangle\eta)^2}\,\frac{\mu_{eff}}{Re}\left(\frac{\partial\eta}{\partial x}\right)^2_i\right] \\
+ \quad & \Psi^{*}_{u\, i}\left[\rho^n_i + 2\,\frac{\triangle t}{(\triangle\eta)^2}\,\frac{\mu_{eff}}{Re}\left(\frac{\partial\eta}{\partial x}\right)^2_i\right] \\
+ \quad & \Psi^{*}_{u\, i+1}\left[\frac{\triangle t}{2\,\triangle\eta}\left(\frac{\partial\eta}{\partial x}\right)_i \rho^n_{i+1}\, u^n_{i+1}\right. \\
& \qquad \left. + \frac{\triangle t}{2\,\triangle\eta}\,\frac{\mu_{eff}}{Re}\left(\frac{\partial^2\eta}{\partial x^2}\right)_i - \frac{\triangle t}{(\triangle\eta)^2}\,\frac{\mu_{eff}}{Re}\left(\frac{\partial\eta}{\partial x}\right)^2_i\right] \\
+ \quad & \Psi^{*}_{T\, i-1}\left[-\frac{\triangle t}{2\,\triangle\eta}\left(\frac{\partial\eta}{\partial x}\right)_i \frac{1}{\gamma\, M^2}\,\rho^n_{i-1}\right] + \Psi^{*}_{T\, i+1}\left[-\frac{\triangle t}{2\,\triangle\eta}\left(\frac{\partial\eta}{\partial x}\right)_i \frac{1}{\gamma\, M^2}\,\rho^n_{i+1}\right] \\
= \quad & -\left[\frac{\triangle t}{2\,\triangle\eta}\left(\frac{\partial\eta}{\partial x}\right)_i\right]\left[\rho^n_{i+1}\left(u^2_{i+1}\right)^n - \rho^n_{i-1}\left(u^2_{i-1}\right)^n\right] \\
& -\left[\frac{\triangle t}{2\,\triangle\zeta}\left(\frac{\partial\zeta}{\partial y}\right)_j\right]\left[\rho^n_{j+1}\, u^n_{j+1}\, v^n_{j+1} - \rho^n_{j-1}\, u^n_{j-1}\, v^n_{j-1}\right] \\
& -\left[\frac{\triangle t}{2\,\triangle\eta}\left(\frac{\partial\eta}{\partial x}\right)_i\right]\left[\frac{1}{\gamma\, M^2}\left(\rho^n_{j+1}\, T^n_{j+1} - \rho^n_{j-1}\, T^n_{j-1}\right)\right] \\
& +\left[\frac{4}{3}\,\frac{\triangle t}{(\triangle\eta)^2}\,\frac{\mu_{eff}}{Re}\left(\frac{\partial\eta}{\partial x}\right)^2_i\right]\left[u^n_{i+1} - 2\,u^n_i + u^n_{i-1}\right] \\
& +\left[\frac{\triangle t}{(\triangle\zeta)^2}\,\frac{\mu_{eff}}{Re}\left(\frac{\partial\zeta}{\partial y}\right)^2_j\right]\left[v^n_{j+1} - 2\,v^n_j + v^n_{j-1}\right] \\
& +\left[\frac{4}{3}\,\frac{\triangle t}{2\,\triangle\eta}\,\frac{\mu_{eff}}{Re}\left(\frac{\partial^2\eta}{\partial x^2}\right)_i\right]\left[u^n_{i+1} - u^n_{i-1}\right] \\
& +\left[\frac{\triangle t}{2\,\triangle\zeta}\,\frac{\mu_{eff}}{Re}\left(\frac{\partial^2\zeta}{\partial y^2}\right)_j\right]\left[v^n_{j+1} - v^n_{j-1}\right]
\end{aligned}
$$

$$+ \left[\frac{1}{3} \frac{\mu_{eff}}{Re} \frac{\Delta t}{4\,\Delta\eta\,\Delta\zeta} \left(\frac{\partial \eta}{\partial x} \right)_i \left(\frac{\partial \zeta}{\partial y} \right)_j \right] \left[v^n_{i+1,j+1} - v^n_{i+1,j-1} - v^n_{i-1,j+1} + v^n_{i-1,j-1} \right] \tag{3.32}$$

After second ADI step

$$\begin{aligned}
& \Psi^{n+1}_{\rho\, j-1} \left[- \frac{\Delta t}{2\,\Delta\zeta} \left(\frac{\partial \zeta}{\partial y} \right)_j u^n_{j-1}\, v^n_{j-1} \right] + \Psi^{n+1}_{\rho j} \left[u^n_j \right] \\
+ \quad & \Psi^{n+1}_{\rho\, j+1} \left[\frac{\Delta t}{2\,\Delta\zeta} \left(\frac{\partial \zeta}{\partial y} \right)_j u^n_{j+1}\, v^n_{j+1} \right] \\
+ \quad & \Psi^{n+1}_{u\, j-1} \left[- \frac{\Delta t}{2\,\Delta\zeta} \left(\frac{\partial \zeta}{\partial y} \right)_j \rho^n_{j-1}\, v^n_{j-1} \right. \\
& \qquad \left. - \frac{\Delta t}{2\,\Delta\zeta} \frac{\mu_{eff}}{Re} \left(\frac{\partial^2 \zeta}{\partial y^2} \right)_j + \frac{\Delta t}{(\Delta\zeta)^2} \frac{\mu_{eff}}{Re} \left(\frac{\partial \zeta}{\partial y} \right)^2_j \right] \\
+ \quad & \Psi^{n+1}_{u\, j} \left[\rho^n_j + 2 \frac{\Delta t}{(\Delta\zeta)^2} \frac{\mu_{eff}}{Re} \left(\frac{\partial \zeta}{\partial y} \right)^2_j \right] \\
+ \quad & \Psi^{n+1}_{u\, j+1} \left[\frac{\Delta t}{2\,\Delta\zeta} \left(\frac{\partial \zeta}{\partial y} \right)_j \rho^n_{j+1}\, v^n_{j+1} \right. \\
& \qquad \left. - \frac{\Delta t}{2\,\Delta\zeta} \frac{\mu_{eff}}{Re} \left(\frac{\partial^2 \zeta}{\partial y^2} \right)_j - \frac{\Delta t}{(\Delta\zeta)^2} \frac{\mu_{eff}}{Re} \left(\frac{\partial \zeta}{\partial y} \right)^2_j \right] \\
+ \quad & \Psi^{n+1}_{v\, j-1} \left[- \frac{\Delta t}{2\,\Delta\zeta} \left(\frac{\partial \zeta}{\partial y} \right)_j \rho^n_{j-1}\, u^n_{j-1} \right] + \Psi^{n+1}_{v\, j+1} \left[\frac{\Delta t}{2\,\Delta\zeta} \left(\frac{\partial \zeta}{\partial y} \right)_j \rho^n_{j+1}\, u^n_{j+1} \right] \\
= \quad & \left[\rho^n_j\, \Psi^*_{u\, j} + u^n_j\, \Psi^*_{\rho\, j} \right]
\end{aligned} \tag{3.33}$$

y-momentum equation :

After first ADI step

$$\begin{aligned}
& \Psi^*_{\rho\, i-1} \left[- \frac{\Delta t}{2\,\Delta\eta} \left(\frac{\partial \eta}{\partial x} \right)_i u^n_{i-1}\, v^n_{i-1} \right] + \Psi^*_{\rho i} \left[v^n_i \right] \\
+ \quad & \Psi^*_{\rho\, i+1} \left[\frac{\Delta t}{2\,\Delta\eta} \left(\frac{\partial \eta}{\partial x} \right)_i u^n_{i+1}\, v^n_{i+1} \right] \\
+ \quad & \Psi^*_{v\, i-1} \left[- \frac{\Delta t}{2\,\Delta\eta} \left(\frac{\partial \eta}{\partial x} \right)_i \rho^n_{i-1}\, u^n_{i-1} \right.
\end{aligned}$$

$$
\begin{aligned}
&- \frac{\Delta t}{2\,\Delta\eta}\,\frac{\mu_{eff}}{Re}\left(\frac{\partial^2\eta}{\partial x^2}\right)_i + \frac{\Delta t}{(\Delta\eta)^2}\,\frac{\mu_{eff}}{Re}\left(\frac{\partial\eta}{\partial x}\right)_i^2\Bigg] \\
&+ \Psi^*_{\rho\,i}\left[\rho^n_i + 2\,\frac{\Delta t}{(\Delta\eta)^2}\,\frac{\mu_{eff}}{Re}\left(\frac{\partial\eta}{\partial x}\right)_i^2\right] \\
&+ \Psi^*_{\rho\,i+1}\left[-\frac{\Delta t}{2\,\Delta\eta}\left(\frac{\partial\eta}{\partial x}\right)_i \rho^n_{i+1}\,u^n_{i+1}\right. \\
&\quad \left. - \frac{\Delta t}{2\,\Delta\eta}\,\frac{\mu_{eff}}{Re}\left(\frac{\partial^2\eta}{\partial x^2}\right)_i + \frac{\Delta t}{(\Delta\eta)^2}\,\frac{\mu_{eff}}{Re}\left(\frac{\partial\eta}{\partial x}\right)_i^2\right] \\
&+ \Psi^*_{u\,i-1}\left[-\frac{\Delta t}{2\,\Delta\eta}\left(\frac{\partial\eta}{\partial x}\right)_i \rho^n_{i-1}\,v^n_{i-1}\right] + \Psi^*_{u\,i+1}\left[\frac{\Delta t}{2\,\Delta\eta}\left(\frac{\partial\eta}{\partial x}\right)_i \rho^n_{i+1}\,u^n_{i+1}\right] \\
=\ &- \left[\frac{\Delta t}{2\,\Delta\eta}\left(\frac{\partial\eta}{\partial x}\right)_i\right]\left[\rho^n_{i+1}\,u^n_{i+1}\,v^n_{i+1} - \rho^n_{i-1}\,u^n_{i-1}\,v^n_{i-1}\right] \\
&- \left[\frac{\Delta t}{2\,\Delta\zeta}\left(\frac{\partial\zeta}{\partial y}\right)_j\right]\left[\rho^n_{j+1}\left(v^2_{j+1}\right)^n - \rho^n_{j-1}\left(v^2_{j-1}\right)^n\right] \\
&+ \left[\frac{\Delta t}{2\,\Delta\zeta}\left(\frac{\partial\zeta}{\partial y}\right)_j\right]\left[\frac{1}{\gamma\,M^2}\left(\rho^n_{j+1}\,T^n_{j+1} - \rho^n_{j-1}\,T^n_{j-1}\right)\right] \\
&+ \left[\frac{4}{3}\,\frac{\Delta t}{(\Delta\zeta)^2}\,\frac{\mu_{eff}}{Re}\left(\frac{\partial\zeta}{\partial y}\right)_j^2\right]\left[v^n_{j+1} - 2\,v^n_j + v^n_{j-1}\right] \\
&+ \left[\frac{4}{3}\,\frac{\Delta t}{2\,\Delta\zeta}\,\frac{\mu_{eff}}{Re}\left(\frac{\partial^2\zeta}{\partial y^2}\right)_j\right]\left[v^n_{j+1} - v^n_{j-1}\right] \\
&+ \left[\frac{\Delta t}{(\Delta\eta)^2}\,\frac{\mu_{eff}}{Re}\left(\frac{\partial\eta}{\partial x}\right)_i^2\right]\left[v^n_{i+1} - 2\,v^n_i + v^n_{i-1}\right] \\
&+ \left[\frac{\Delta t}{2\,\Delta\eta}\,\frac{\mu_{eff}}{Re}\left(\frac{\partial^2\eta}{\partial x^2}\right)_i\right]\left[v^n_{i+1} - v^n_{i-1}\right] \\
&+ \left[\frac{1}{3}\,\frac{\mu_{eff}}{Re}\,\frac{\Delta t}{4\,\Delta\eta\,\Delta\zeta}\left(\frac{\partial\eta}{\partial x}\right)_i\left(\frac{\partial\zeta}{\partial y}\right)_j\right] \\
&\left[u^n_{i+1,j+1} - u^n_{i+1,j-1} - u^n_{i-1,j+1} + u^n_{i-1,j-1}\right] \qquad (3.34)
\end{aligned}
$$

After second ADI step

$$
\Psi^{n+1}_{\rho\,j-1}\left[-\frac{\Delta t}{2\,\Delta\zeta}\left(\frac{\partial\zeta}{\partial y}\right)_j\left(v^2_{j-1}\right)^n + \frac{1}{\gamma\,M^2}\,T^n_{j-1}\right] + \Psi^{n+1}_{\rho\,j}\left[v^n_j\right]
$$

$$
\begin{aligned}
&+ \quad \Psi^{n+1}_{v\,j+1} \left[\frac{\triangle t}{2\,\triangle\zeta} \left(\frac{\partial \zeta}{\partial y} \right)_j \left(v^2_{j+1} \right)^n + \frac{1}{\gamma\, M^2}\, T^n_{j+1} \right] \\
&+ \quad \Psi^{n+1}_{v\,j-1} \left[-\, 2\, \frac{\triangle t}{2\,\triangle\zeta} \left(\frac{\partial \zeta}{\partial y} \right)_j \rho^n_{j-1}\; v^n_{j-1} \right. \\
&\qquad \left. + \frac{\triangle t}{2\,\triangle\zeta}\, \frac{\mu_{eff}}{Re} \left(\frac{\partial^2 \zeta}{\partial y^2} \right)_j - \frac{\triangle t}{(\triangle\zeta)^2}\, \frac{\mu_{eff}}{Re} \left(\frac{\partial \zeta}{\partial y} \right)^2_j \right] \\
&+ \quad \Psi^{n+1}_{v\,j} \left[\rho^n_j + 2\, \frac{\triangle t}{(\triangle\zeta)^2}\, \frac{\mu_{eff}}{Re} \left(\frac{\partial \zeta}{\partial y} \right)^2_j \right] \\
&+ \quad \Psi^{n+1}_{v\,j+1} \left[2\, \frac{\triangle t}{2\,\triangle\zeta} \left(\frac{\partial \zeta}{\partial y} \right)_j \rho^n_{j+1}\; v^n_{j+1} \right. \\
&\qquad \left. - \frac{\triangle t}{2\,\triangle\zeta}\, \frac{\mu_{eff}}{Re} \left(\frac{\partial^2 \zeta}{\partial y^2} \right)_j - \frac{\triangle t}{(\triangle\zeta)^2}\, \frac{\mu_{eff}}{Re} \left(\frac{\partial \zeta}{\partial y} \right)^2_j \right] \\
&+ \quad \Psi^{n+1}_{T\,j-1} \left[-\, \frac{\triangle t}{2\,\triangle\zeta} \left(\frac{\partial \zeta}{\partial y} \right)_j \frac{1}{\gamma\, M^2}\, \rho^n_{j-1} \right] + \Psi^{n+1}_{T\,j+1} \left[\frac{\triangle t}{2\,\triangle\zeta} \left(\frac{\partial \zeta}{\partial y} \right)_j \frac{1}{\gamma\, M^2}\, \rho^n_{j+1} \right] \\
&= \quad \left[\rho^n_j\; \Psi^{\star}_{v\,j} + v^n_j\; \Psi^{\star}_{\rho\,j} \right] \qquad (3.35)
\end{aligned}
$$

Energy equation :

After first ADI step

$$
\begin{aligned}
&\qquad \Psi^{\star}_{\rho\,i-1} \left[-\, \frac{\triangle t}{2\,\triangle\eta} \left(\frac{\partial \eta}{\partial x} \right)_i u^n_{i-1}\; T^n_{i-1} \right] \\
&+ \quad \Psi^{\star}_{\rho\,i} \left[T^n_i \left(1 + \frac{\triangle t}{2\,\triangle\eta} \left(\frac{\partial \eta}{\partial x} \right)_i (\gamma - 1)\, (u^n_{i+1} - u^n_{i-1}) \right) \right] \\
&+ \quad \Psi^{\star}_{\rho\,i+1} \left[\frac{\triangle t}{2\,\triangle\eta} \left(\frac{\partial \eta}{\partial x} \right)_i u^n_{i+1}\; T^n_{i+1} \right] \\
&+ \quad \Psi^{\star}_{T\,i-1} \left[-\, \frac{\triangle t}{2\,\triangle\eta} \left(\frac{\partial \eta}{\partial x} \right)_i \rho^n_{i-1}\; u^n_{i-1} \right. \\
&\qquad \left. - \frac{\gamma\, k_{eff}}{Re\, Pr}\, \frac{\triangle t}{(\triangle\eta)^2} \left(\frac{\partial \eta}{\partial x} \right)^2_i + \frac{\gamma\, k_{eff}}{Re\, Pr}\, \frac{\triangle t}{2\,\triangle\eta} \left(\frac{\partial^2 \eta}{\partial x^2} \right)_i \right] \\
&+ \quad \Psi^{\star}_{T\,i} \left[\rho^n_i + 2\, \frac{\gamma\, k_{eff}}{Re\, Pr}\, \frac{\triangle t}{(\triangle\eta)^2} \left(\frac{\partial \eta}{\partial x} \right)^2_i \right. \\
&\qquad \left. + \frac{\triangle t}{2\,\triangle\eta} \left(\frac{\partial \eta}{\partial x} \right)_i (\gamma - 1)\, \rho^n_i\, (u^n_{i+1} - u^n_{i-1}) \right]
\end{aligned}
$$

$$
\begin{aligned}
&+ \quad \Psi^{*}_{T\,i+1} \left[- \frac{\Delta t}{2\,\Delta\eta} \left(\frac{\partial \eta}{\partial x} \right)_i \rho^n_{i+1}\; T^n_{i+1} \right. \\
&\qquad \left. - \frac{\gamma\, k_{eff}}{Re\; Pr} \frac{\Delta t}{(\Delta\eta)^2} \left(\frac{\partial \eta}{\partial x} \right)^2_i - \frac{\gamma\, k_{eff}}{Re\; Pr} \frac{\Delta t}{2\,\Delta\eta} \left(\frac{\partial^2 \eta}{\partial x^2} \right)_i \right] \\
&+ \quad \Psi^{*}_{u\,i-1} \left[- \frac{\Delta t}{2\,\Delta\eta} \left(\frac{\partial \eta}{\partial x} \right)_i \left(\rho^n_{i-1}\; T^n_{i-1} - (\gamma - 1)\; \rho^n_i\; T^n_i \right) \right] \\
&+ \quad \Psi^{*}_{u\,i+1} \left[\frac{\Delta t}{2\,\Delta\eta} \left(\frac{\partial \eta}{\partial x} \right)_i \left(\rho^n_{i-1}\; T^n_{i-1} + (\gamma - 1)\; \rho^n_i\; T^n_i \right) \right] \\
&= \quad - \left[\frac{\Delta t}{2\,\Delta\eta} \left(\frac{\partial \eta}{\partial x} \right)_i \right] \left[\rho^n_{i+1}\; u^n_{i+1}\; T^n_{i+1} - \rho^n_{i-1}\; u^n_{i-1}\; T^n_{i-1} \right] \\
&\quad - \left[\frac{\Delta t}{2\,\Delta\zeta} \left(\frac{\partial \zeta}{\partial y} \right)_j \right] \left[\rho^n_{j+1}\; v^n_{j+1}\; T^n_{j+1} - \rho^n_{j-1}\; v^n_{j-1}\; T^n_{j-1} \right] \\
&\quad + \left[\frac{\gamma\, k_{eff}}{Re\; Pr} \frac{\Delta t}{(\Delta\eta)^2} \left(\frac{\partial \eta}{\partial x} \right)^2_i \right] \left[T^n_{i+1} - 2\,T^n_i + T^n_{i-1} \right] \\
&\quad + \left[\frac{\gamma\, k_{eff}}{Re\; Pr} \frac{\Delta t}{2\,\Delta\eta} \left(\frac{\partial^2 \eta}{\partial x^2} \right)_i \right] \left[T^n_{i+1} - T^n_{i-1} \right] \\
&\quad + \left[\frac{\gamma\, k_{eff}}{Re\; Pr} \frac{\Delta t}{(\Delta\zeta)^2} \left(\frac{\partial \zeta}{\partial y} \right)^2_j \right] \left[T^n_{j+1} - 2\,T^n_j + T^n_{j-1} \right] \\
&\quad + \left[\frac{\gamma\, k_{eff}}{Re\; Pr} \frac{\Delta t}{2\,\Delta\zeta} \left(\frac{\partial^2 \zeta}{\partial y^2} \right)_j \right] \left[T^n_{j+1} - T^n_{j-1} \right] \\
&\quad + \left[\Delta t\, \gamma\, (\gamma - 1)\; M^2\, \frac{\mu_{eff}}{Re} \right] \\
&\left[2 \left\{ \left(\frac{1}{2\,\Delta\eta} \left(\frac{\partial \eta}{\partial x} \right)_i \left(u^n_{i+1} - u^n_{i-1} \right) \right)^2 + \left(\frac{1}{2\,\Delta\zeta} \left(\frac{\partial \zeta}{\partial y} \right)_j \left(v^n_{j+1} - v^n_{j-1} \right) \right)^2 \right\} \right. \\
&\quad + \left\{ \frac{1}{2\,\Delta\eta} \left(\frac{\partial \eta}{\partial x} \right)_i \left(v^n_{i+1} - v^n_{i-1} \right) + \frac{1}{2\,\Delta\zeta} \left(\frac{\partial \zeta}{\partial y} \right)_j \left(u^n_{j+1} - u^n_{j-1} \right) \right\}^2 \\
&\quad \left. + \frac{2}{3} \left\{ \frac{1}{2\Delta\eta} \left(\frac{\partial \eta}{\partial x} \right)_i \left(u^n_{i+1} - u^n_{i-1} \right) + \frac{1}{2\,\Delta\zeta} \left(\frac{\partial \zeta}{\partial y} \right)_j \left(v^n_{j+1} - v^n_{j-1} \right) \right\}^2 \right] \\
&- \left[\Delta t\; (\gamma - 1)\; \rho^n_i\; T^n_i \right] \\
&\left[\frac{\Delta t}{2\,\Delta\eta} \left(\frac{\partial \eta}{\partial x} \right)_i \left(u^n_{i+1} - u^n_{i-1} \right) + \frac{\Delta t}{2\,\Delta\zeta} \left(\frac{\partial \zeta}{\partial y} \right)_j \left(v^n_{j+1} - v^n_{j-1} \right) \right] \qquad (3.3
\end{aligned}
$$

After second ADI step

$$
\begin{aligned}
& \Psi^{n+1}_{\rho\, j-1} \left[-\frac{\Delta t}{2\,\Delta\eta} \left(\frac{\partial \eta}{\partial x} \right)_i \; u^n_{j-1} \; T^n_{j-1} \right] \\
+ \quad & \Psi^{n+1}_{\rho\, j} \left[T^n_j \left(1 + \frac{\Delta t}{2\,\Delta\zeta} \left(\frac{\partial \zeta}{\partial y} \right)_j (\gamma - 1) \left(v^n_{j+1} - v^n_{j-1} \right) \right) \right] \\
+ \quad & \Psi^{n+1}_{\rho\, j+1} \left[\frac{\Delta t}{2\,\Delta\eta} \left(\frac{\partial \eta}{\partial x} \right)_i \; v^n_{j+1} \; T^n_{j+1} \right] \\
+ \quad & \Psi^{n+1}_{T\, j-1} \left[-\frac{\Delta t}{2\,\Delta\eta} \left(\frac{\partial \eta}{\partial x} \right)_i \; \rho^n_{j-1} \; v^n_{j-1} \right. \\
& \qquad \left. - \frac{\gamma\, k_{eff}}{Re\, Pr} \frac{\Delta t}{(\Delta\zeta)^2} \left(\frac{\partial \zeta}{\partial y} \right)^2_j + \frac{\gamma\, k_{eff}}{Re\, Pr} \frac{\Delta t}{2\,\Delta\zeta} \left(\frac{\partial^2 \zeta}{\partial y^2} \right)_j \right] \\
+ \quad & \Psi^{n+1}_{T\, j} \left[\rho^n_j + 2\, \frac{\gamma\, k_{eff}}{Re\, Pr} \frac{\Delta t}{(\Delta\zeta)^2} \left(\frac{\partial \zeta}{\partial y} \right)^2_j \right. \\
& \qquad \left. + \frac{\Delta t}{2\,\Delta\zeta} \left(\frac{\partial \zeta}{\partial y} \right)_j (\gamma - 1)\, \rho^n_j \left(v^n_{j+1} - v^n_{j-1} \right) \right] \\
+ \quad & \Psi^{n+1}_{T\, j+1} \left[-\frac{\Delta t}{2\,\Delta\zeta} \left(\frac{\partial \zeta}{\partial y} \right)_j \; \rho^n_{j+1} \; T^n_{i+1} \right. \\
& \qquad \left. - \frac{\gamma\, k_{eff}}{Re\, Pr} \frac{\Delta t}{(\Delta\zeta)^2} \left(\frac{\partial \zeta}{\partial y} \right)^2_j - \frac{\gamma\, k_{eff}}{Re\, Pr} \frac{\Delta t}{2\,\Delta\zeta} \left(\frac{\partial^2 \zeta}{\partial y^2} \right)_j \right] \\
+ \quad & \Psi^{n+1}_{v\, j-1} \left[-\frac{\Delta t}{2\,\Delta\zeta} \left(\frac{\partial \zeta}{\partial y} \right)_j \left(\rho^n_{j-1} \; T^n_{j-1} - (\gamma - 1)\, \rho^n_i \; T^n_i \right) \right] \\
+ \quad & \Psi^{n+1}_{v\, j+1} \left[\frac{\Delta t}{2\,\Delta\zeta} \left(\frac{\partial \zeta}{\partial y} \right)_j \left(\rho^n_{j-1} \; T^n_{j-1} + (\gamma - 1)\, \rho^n_j \; T^n_j \right) \right] \\
= \quad & \left[\rho^n_j \; \Psi^*_{T\, j} + T^n_j \; \Psi^*_{\rho\, j} \right]
\end{aligned}
\tag{3.37}
$$

3.4 Discretised Boundary Conditions

Along the wall, $\zeta = 1$;

$$
\Psi^{n+1}_{u\, i,1} = \Psi^{n+1}_{v\, i,1} = 0 \tag{3.38}
$$

$$
\Psi^{n+1}_{T\, i,1} = \frac{4}{3}\, \Psi^{n+1}_{T\, i,2} - \frac{1}{3}\, \Psi^{n+1}_{T\, i,3} - T^n_{i,2} + \frac{4}{3}\, T^n_{i,2} - \frac{1}{3}\, T^n_{i,3} \tag{3.39}
$$

The boundary condition for density is obtained as follows.

$$\frac{\partial \rho}{\partial t} + \frac{\partial}{\partial y}(\rho v)^{n+1} = 0 \tag{3.40}$$

After expanding the nonlinear terms, transforming and discretizing the above equation becomes

$$\begin{aligned}\Psi_{\rho\, i,1}^{n+1} = & -\frac{\Delta t}{2\,\Delta\zeta}\left(\frac{\partial \zeta}{\partial y}\right)_1 \Big[4\, v_{i,2}^{n}\ \Psi_{\rho\, i,2}^{n+1} + 4\,\rho_{i,2}^{n}\ \Psi_{v\, i,2}^{n+1} - v_{i,2}^{n}\ \Psi_{\rho\, i,3}^{n+1} \\ & - \rho_{i,2}^{n}\ \Psi_{v\, i,3}^{n+1} - 4\,\rho_{i,2}^{n}\ v_{i,2}^{n} + \rho_{i,3}^{n}\ v_{i,3}^{n}\Big]\end{aligned} \tag{3.41}$$

Along the free stream boundary, $\zeta = \zeta_{max}$:

$$\Psi_{u\, i,ny}^{n+1} = \Psi_{v\, i,ny}^{n+1} = \Psi_{\rho\, i,ny}^{n+1} = \Psi_{T\, i,ny}^{n+1} = 0 \tag{3.42}$$

$$\begin{aligned}\Psi_{\rho\, i,ny-1}^{n+1} &= \frac{1}{2}\Psi_{\rho\, i,ny-2}^{n+1}\,; \quad \Psi_{u\, i,ny-1}^{n+1} = \frac{1}{2}\Psi_{u\, i,ny-2}^{n+1} \\ \Psi_{v\, i,ny-1}^{n+1} &= \frac{1}{2}\Psi_{v\, i,ny-2}^{n+1}\,; \quad \Psi_{T\, i,ny-1}^{n+1} = \frac{1}{2}\Psi_{T\, i,ny-2}^{n+1}\end{aligned} \tag{3.43}$$

Along the upstream boundary, $\eta = 1$:

$$\Psi_{u\, i,1}^{n+1} = \Psi_{v\, i,1}^{n+1} = \Psi_{\rho\, i,1}^{n+1} = \Psi_{T\, i,1}^{n+1} = 0 \tag{3.44}$$

Along the downstream boundary : $\eta = \eta_{max}$

$$\begin{aligned}\Psi_{u\, nx,j}^{n+1} &= \frac{c2}{c1}\Psi_{u\, nx-1,j}^{n+1} - \frac{c3}{c1}\Psi_{u\, nx-2,j}^{n+1} - u_{nx,j}^{n} + \frac{c2}{c1}u_{nx-1,j}^{n} - \frac{c3}{c1}u_{nx-2,j}^{n} \\ \Psi_{v\, nx,j}^{n+1} &= \frac{c2}{c1}\Psi_{v\, nx-1,j}^{n+1} - \frac{c3}{c1}\Psi_{v\, nx-2,j}^{n+1} - v_{nx,j}^{n} + \frac{c2}{c1}v_{nx-1,j}^{n} - \frac{c3}{c1}v_{nx-2,j}^{n} \\ \Psi_{T\, nx,j}^{n+1} &= \frac{c2}{c1}\Psi_{T\, nx-1,j}^{n+1} - \frac{c3}{c1}\Psi_{T\, nx-2,j}^{n+1} - T_{nx,j}^{n} + \frac{c2}{c1}T_{nx-1,j}^{n} - \frac{c3}{c1}T_{nx-2,j}^{n}\end{aligned}$$

where

$$\begin{aligned}c1 &= \left[\frac{1}{(\Delta\eta)^2}\left(\frac{\partial \eta}{\partial x}\right)_{nx}^{2} + \frac{3}{2\,\Delta\eta}\left(\frac{\partial^2 \eta}{\partial x^2}\right)_{nx}\right] \\ c2 &= \left[\frac{2}{(\Delta\eta)^2}\left(\frac{\partial \eta}{\partial x}\right)_{nx}^{2} + \frac{4}{2\,\Delta\eta}\left(\frac{\partial^2 \eta}{\partial x^2}\right)_{nx}\right] \\ c3 &= \left[\frac{1}{(\Delta\eta)^2}\left(\frac{\partial \eta}{\partial x}\right)_{nx}^{2} + \frac{1}{2\,\Delta\eta}\left(\frac{\partial^2 \eta}{\partial x^2}\right)_{nx}\right]\end{aligned} \tag{3.45}$$

For density

$$\rho^n_{nx,j}\ \Psi^{n+1}_{T\,nx,j} + T^n_{nx,j}\ \Psi^{n+1}_{\rho\,nx,j} = 0 \tag{3.46}$$

It can be observed from the above set of discretized equations that, during first ADI step, the continuity equation, x-momentum equation and energy equations are only coupled and the y-momentum equation is decoupled from the other equations. Similarly, during second ADI step the continuity equation, the y-momentum equation and energy equations are coupled and the x-momentum equation is decoupled from the other equations.

During the first ADI step, the coupled continuity equation , x-momentum equation and energy equations along with corresponding boundary conditions for ρ, u, and T form a 3×3 block tridiagonal algebraic equations and can be solved for Ψ^*_ρ , Ψ^*_u and Ψ^*_T [8]. The decoupled y-momentum equation and the boundary condition for v form a simple tridiagonal algebraic equations and can be solved for Ψ^*_v .

Similarly, during the second ADI step, Ψ^{n+1}_ρ , Ψ^{n+1}_v and Ψ^{n+1}_T can be obtained by solving a set of coupled equations, and Ψ^{n+1}_u can be obtained independently.

Further, the solution at $n+1$ time level is used for updating the turbulent viscosity. This procedure is repeated until the steady state solution is achieved.

Chapter 4

Results and Discussion

The numerical scheme as described in the earlier chapters has been implemented to analyse the flow over the thin flat plate by solving the ensemble-averaged Navier-Stokes equations. A computer code has been developed and tested with the available experimental data for both laminar and turbulent regions.

Firstly the laminar flow is analysed for a low temperature, low Mach no. subsonic flow. Such a low Mach no. flow behaves almost incompressible and the code prediction can be compared with the Blasius solution. A plot of u vs η_B(where η_B is equal to $y\sqrt{\frac{\rho_\infty u_\infty}{\mu x}}$ as in Blasius solution) is shown in Figure 4.1. The v vs η_B and T vs η_B are plotted in Figure 4.2 and Figure 4.3 respectively. The coefficient of skin friction C_f vs Re_x is plotted in Figure 4.4. There is little variation in temperature T and velocity v and can be observed from the corresponding plots. Some minor fluctuations within 2 to 3 % are observed in the results and can be attributed to numerical oscillations. The variation of density is very little and can be negligible. The matching of the curves u vs η_B and C_f vs Re_x with the known Blasius solution validate the code. The input parameters for this comparison of laminar flow are as follows.

L	=	1.0 ;	y_{max}	=	0.125
N_x	=	21	N_y	=	21
σ_x	=	0.99 ;	σ_y	=	0.001
M	=	0.0718 ;	Re_L	=	3.3×10^5
Pr	=	0.72			

The value of σ_x is taken as 0.99, which produces almost uniform grids in x-

direction, whereas σ_y is taken as 0.001, which cluster the grid points near the wall in y-direction as shown in Figure 2.2. The time step is chosen initially such that the CFL no. is equal to 2 and gradually changed to 20. Further higher CFL nos. lead to numerical oscillations in the solutions. The computation is stopped by checking the difference between two consecutive solutions at grid point ($\mathbf{N}x/2, 4$) till it becomes less than the stipulated accuracy. The total number of time steps to get the steady state within the accuracy of 0.000001 is found to be 180 for the above set of input parameters.

There can be some error in the solution near the upstream boundary and near the down stream boundary, due to the leading edge singularity and to the modelling the down stream boundary conditions. About 4 grid points on the either end, the result can be suspected to be erroneous to some extent.

While analysing the laminar flow field, the turbulent viscosity is set to zero. It is observed that there is no need of the artificial viscosity and fourth order damping for the laminar flow.

Next the turbulent region is analysed starting from leading edge (including the laminar and transition regions). A zero-equation turbulence model developed by Cebeci and Smith [8] is used for the turbulent viscosity in the turbulent zone. The transition is considered by taking an empirical expression for intermittency factor as discussed earlier in section 2.6. The code prediction is compared with the Simpson's [24] experimental data for the mean velocity profiles with the following set of input parameters.

L	=	1.0 ;	y_{max}	=	0.055
N_x	=	51	N_y	=	51
σ_x	=	0.99 ;	σ_y	=	0.001
M	=	0.038 ;	Re_L	=	2.0×10^6
Pr	=	0.72			

The transition is assumed to occur at $Re_x = 4 \times 10^5$ [24], the CFL no. of about 10 is achieved for this calculation starting with 2 initially. The check for the steady state is made as explained as earlier. The result along with the Simpson's [24] experimental data are shown in the Figure 4.5. This comparison validates the code for the turbulent flow region.

The code is then used for 3 sets of input parameters to see the behaviour of code prediction. The various input parameters for these test runs are given below.

Parameter	Run 1	Run 2	Run 3
L	1	1	1
y_{max}	0.055	0.055	0.055
Grid points	51×51	51×51	101×101
Re_L	7.5×10^6	6.0×10^6	1.0×10^7
M	0.36	0.28	0.5
Pr	0.72	0.72	0.72

The Re_{xtr} no. is taken as 4×10^6 as before for all the cases. To develop the solution, the CFL no. is initially taken as 2 and then gradually increased to 10. The total no. of time steps are found to be about 600 to get steady state.

The C_f vs Re_x for all these 3 runs are plotted in Figure 4.6 along with the empirical correlation given in Schlichting [22] and $\log C_f$ vs $\log Re_x$ plot is given in Figure 4.7. The correlation is restricted to a certain range of Reynolds no. but without any specification of the transition Reynolds no, Mach no., and Prandtl no.. However in spite of some minor differences between the predicted and empirical relation of the C_f with Re_x, in view of the earlier comparison of velocity profile with Simpson's [24] experimental data, it can be concluded that the code predictions are reasonably accurate.

The variation of mean velocity u with y for various Re_x numbers (at various locations on the plate for a single run, Run 3) are shown in Figure 4.8. Similarly the variations in mean temperature T and mean normal velocity v with y are plotted in Figures 4.9. and 4.10 respectively. There occurs rise in temperature in the downstream direction due to viscous effects and can be seen in the Figure 4.9. The mean velocity v is becoming zero as the upstream boundary approaches. The minor oscillations can be attributed to numerical errors.

The behaviour of the turbulence model, ie. the variation of the turbulent viscosity for Run 3, at $Re_x = 5 \times 10^6$ is plotted in Figure. 4 .11. Until the point A the turbulent viscosity is obtained from the inner layer expression and then from the A to B the outer layer expression is used as described in section 2.6. The convergence history of the velocity u with time at a grid point (51,4) for the Run 3 is shown in the Figure 4 .12. In order to develop the mean velocity gradients, the turbulent viscosity model is introduced after some time steps (presently, after 50 time steps). A sudden rise in the velocity can be observed due to this.

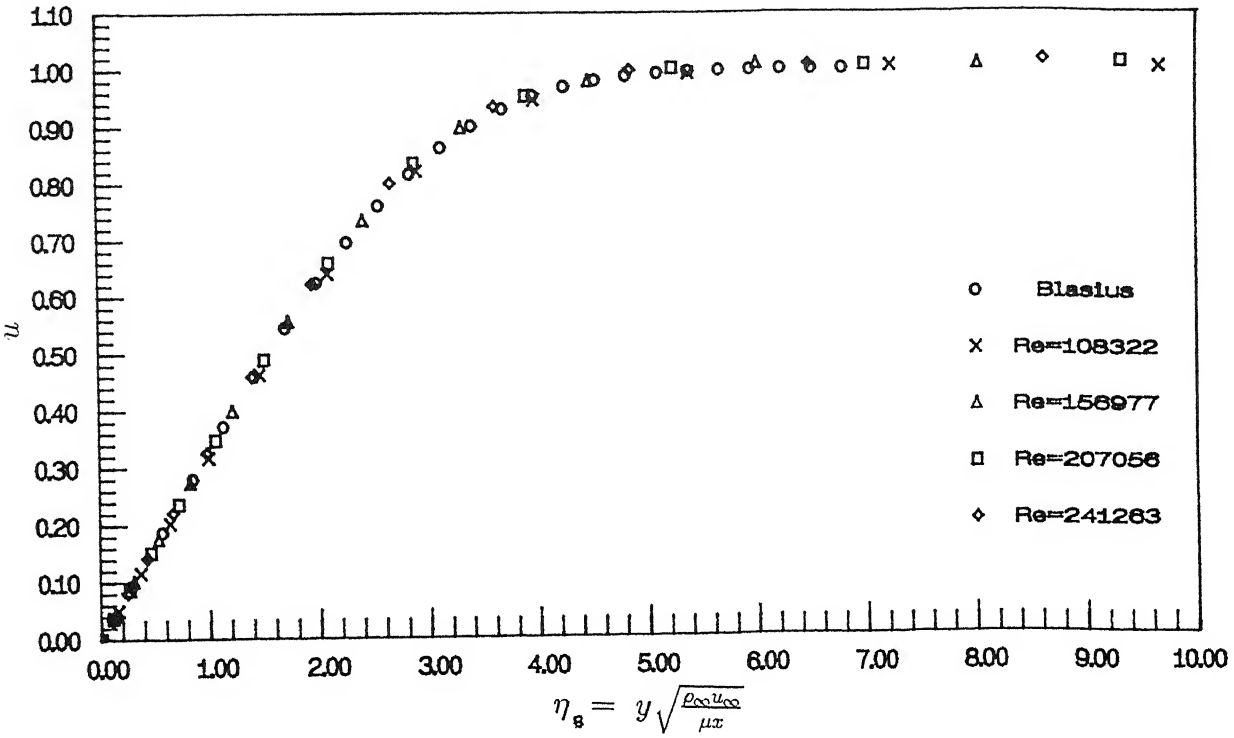

Figure 4.1: Comparison with Blasius Solution.

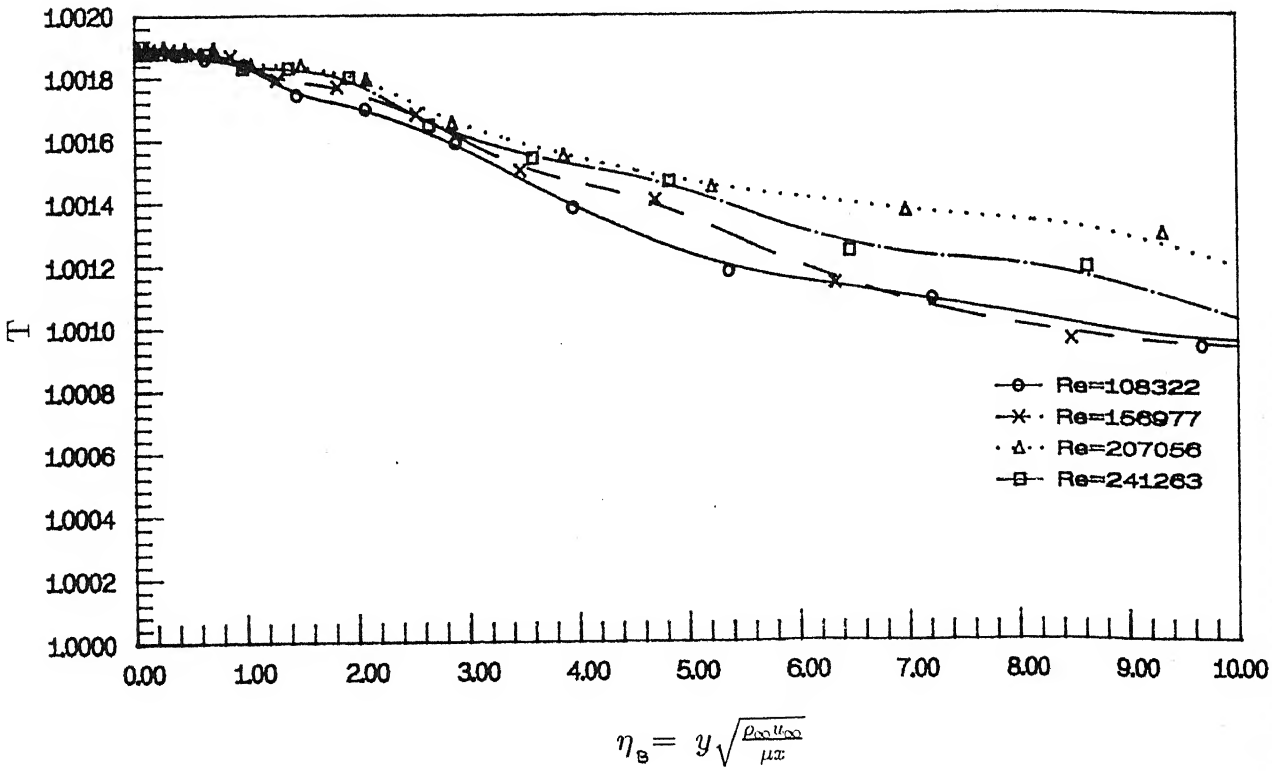

Figure 4.2: Temperature Profiles for Laminar Case.

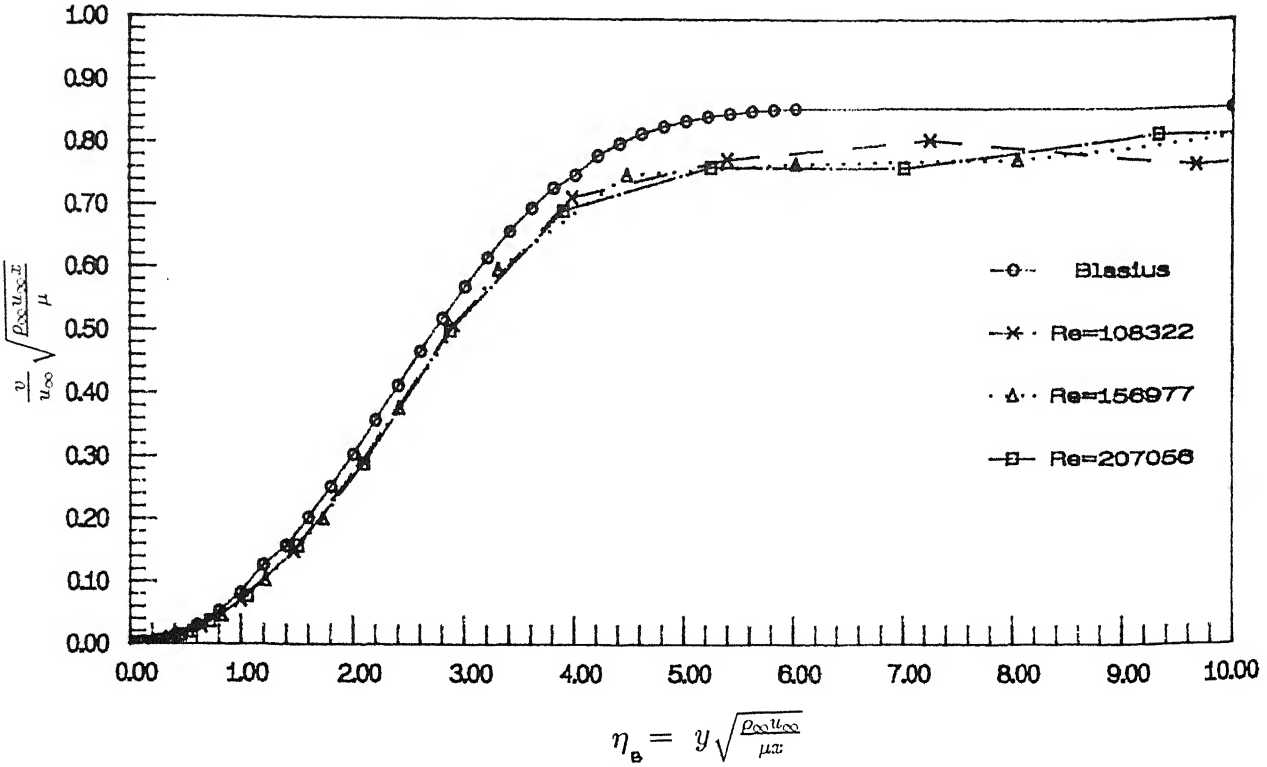

Figure 4.3: v Velocity Profiles for Laminar Case.

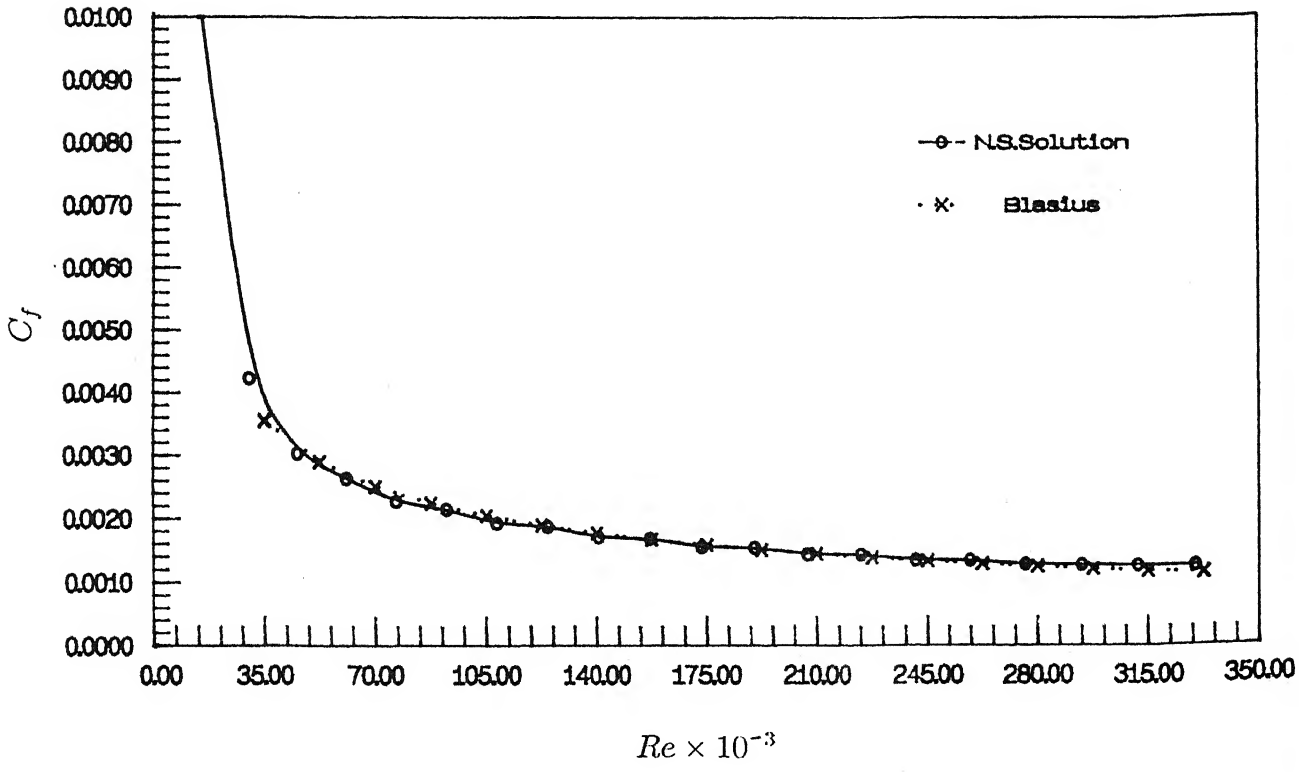

Figure 4.4: Local Skin Friction Coefficient vs Re_x for Laminar case

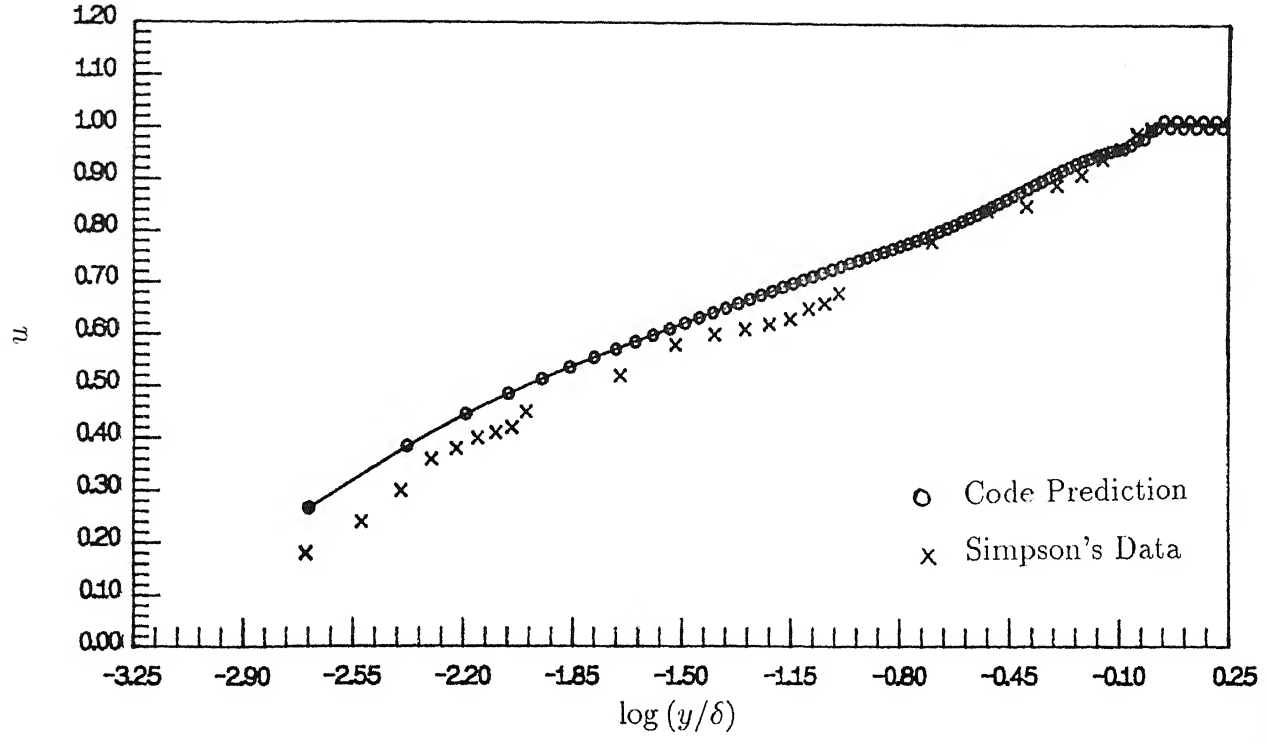

Figure 4.5: Comparison with Simpson's Experimental Data at $Re_x = 1 \times 10^6$

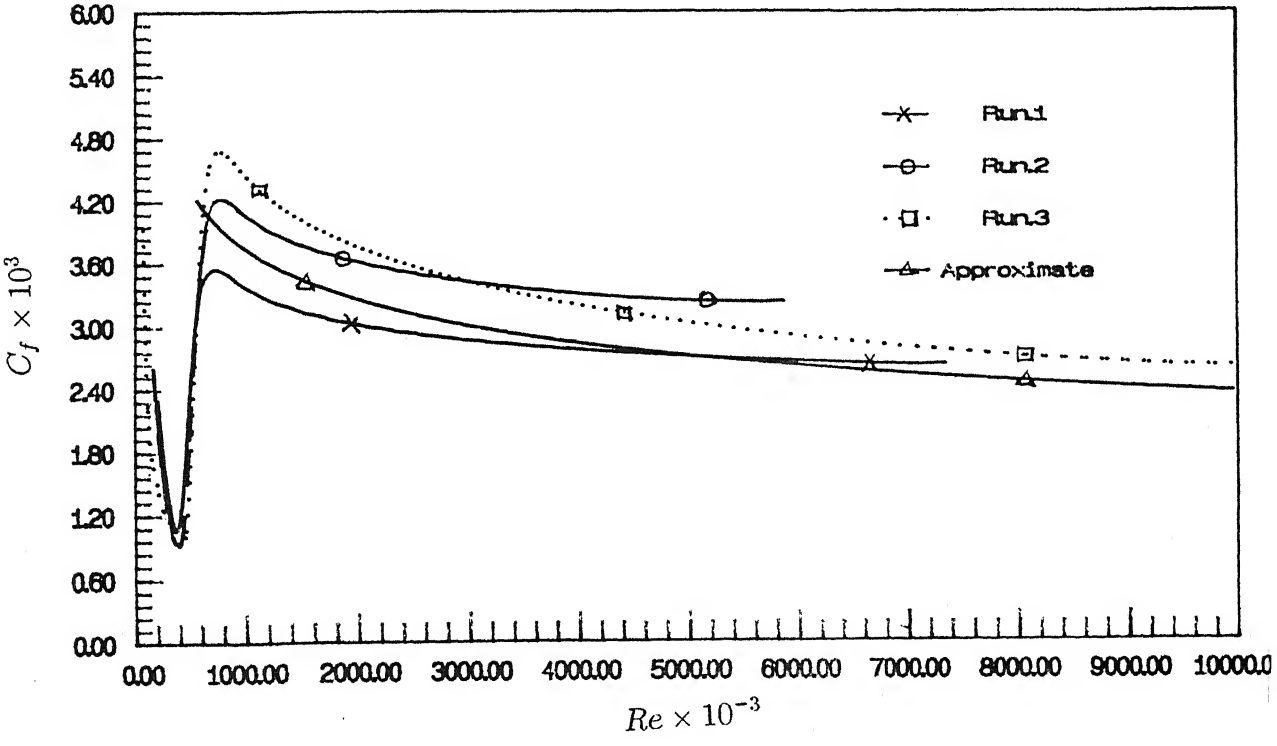

Figure 4.6: Local Skin Friction Coefficient vs Re_x For Turbulent Flow

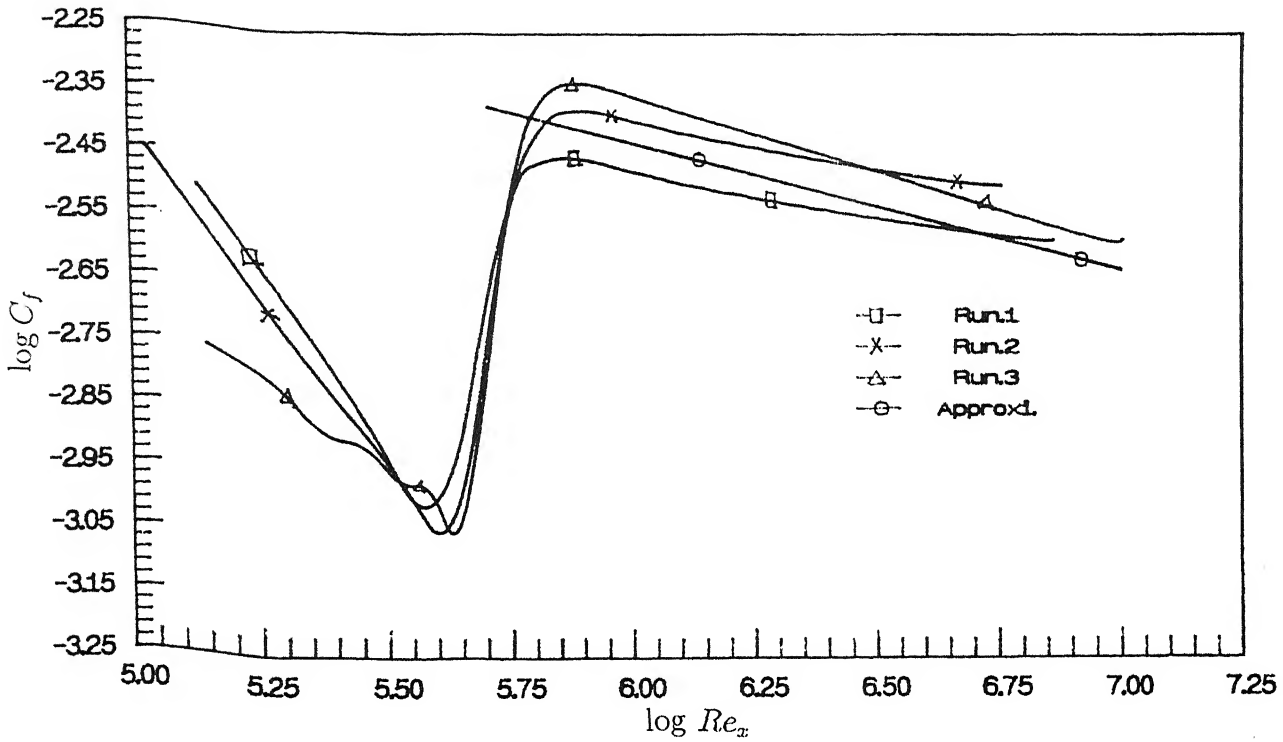

Figure 4.7: Log Local Skin Friction Coefficient vs Log Re_x – For Turbulent Flow

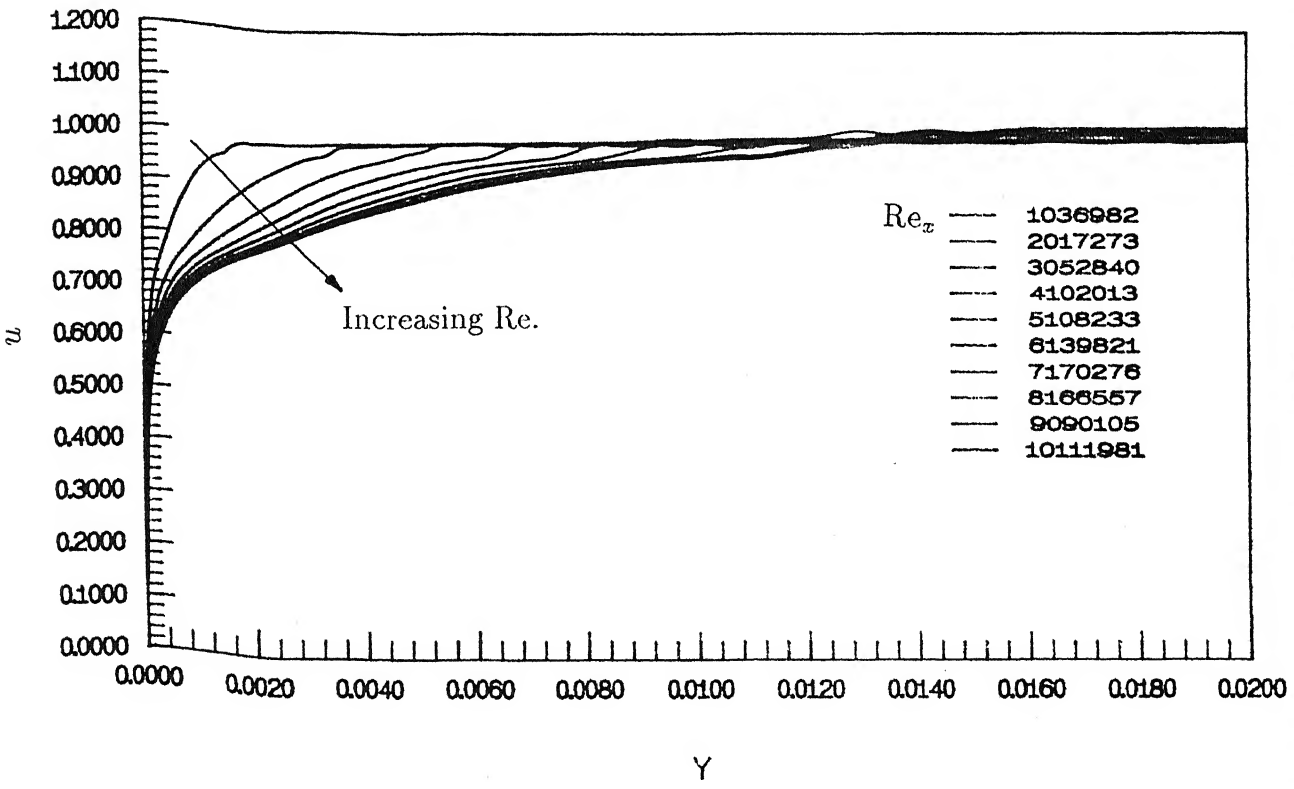

Figure 4.8: Mean u Velocity Profiles at Different Re_x – For Turbulent Flow

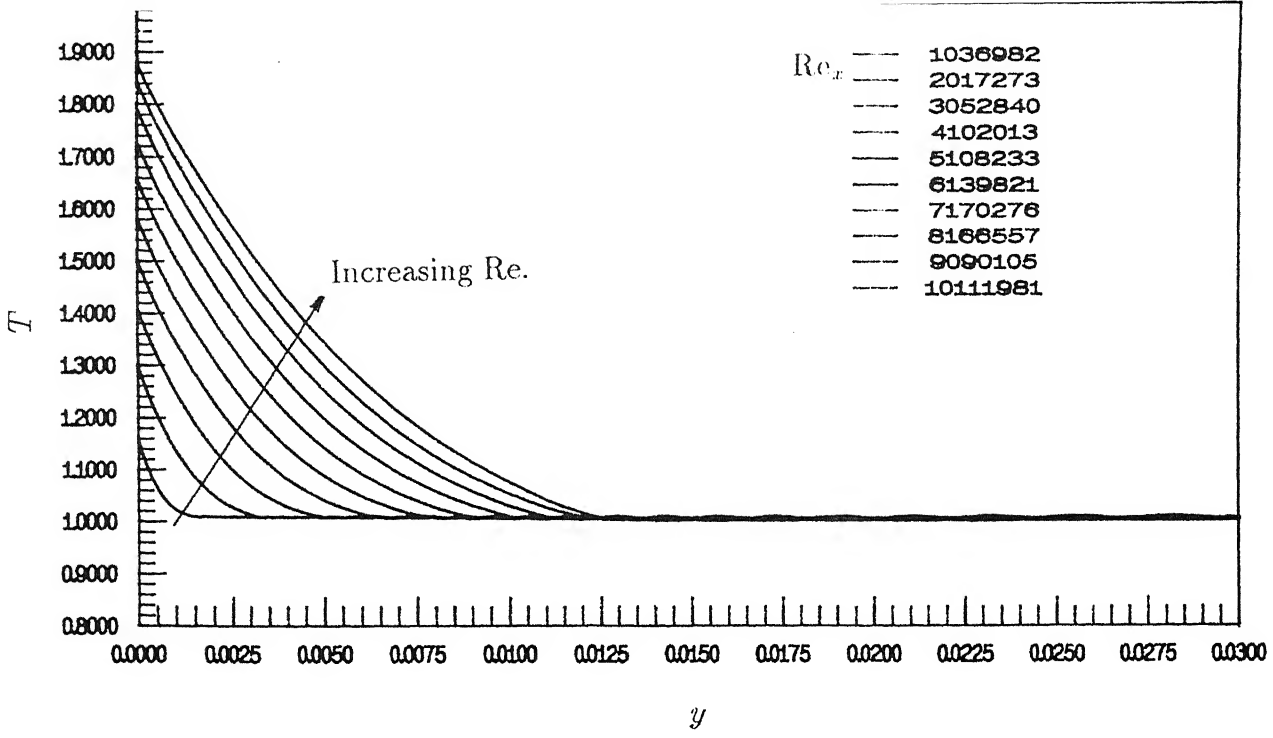

4.9 Mean T Temperature Profiles at Different Re_x- For turbulent flow.

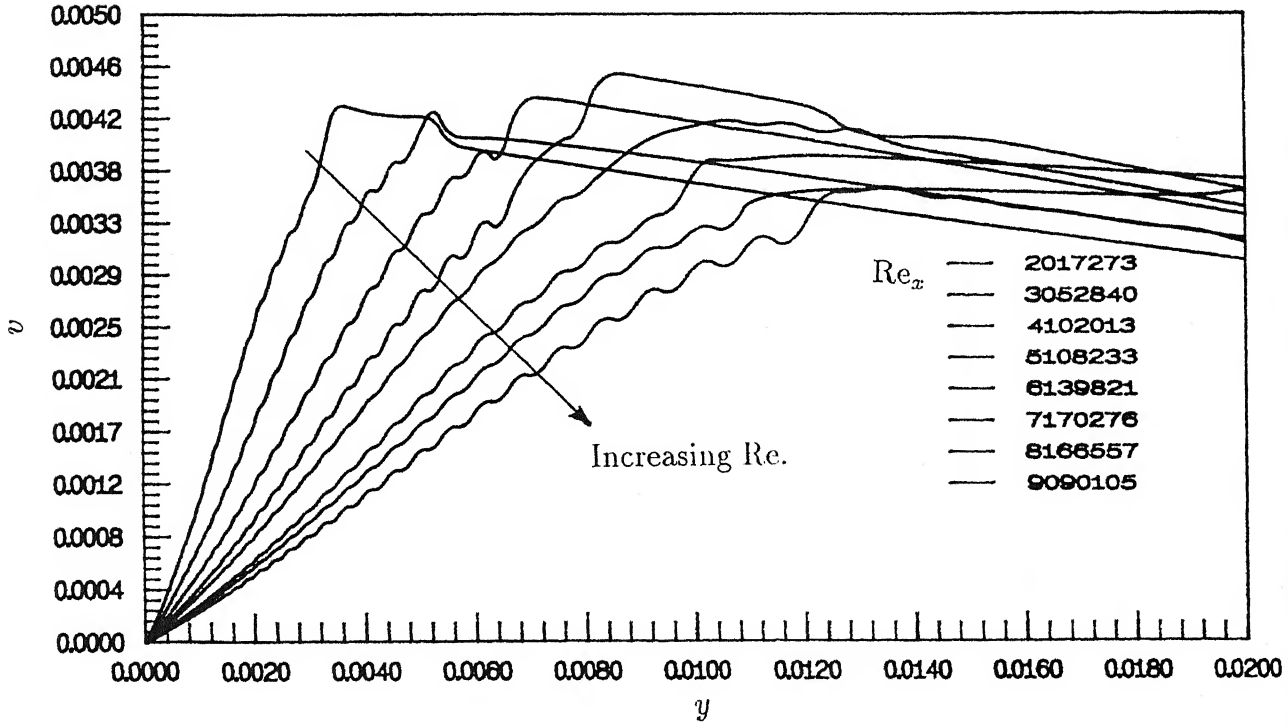

4.10 Mean v Velocity Profiles at Different Re_x For Turbulent Flow.

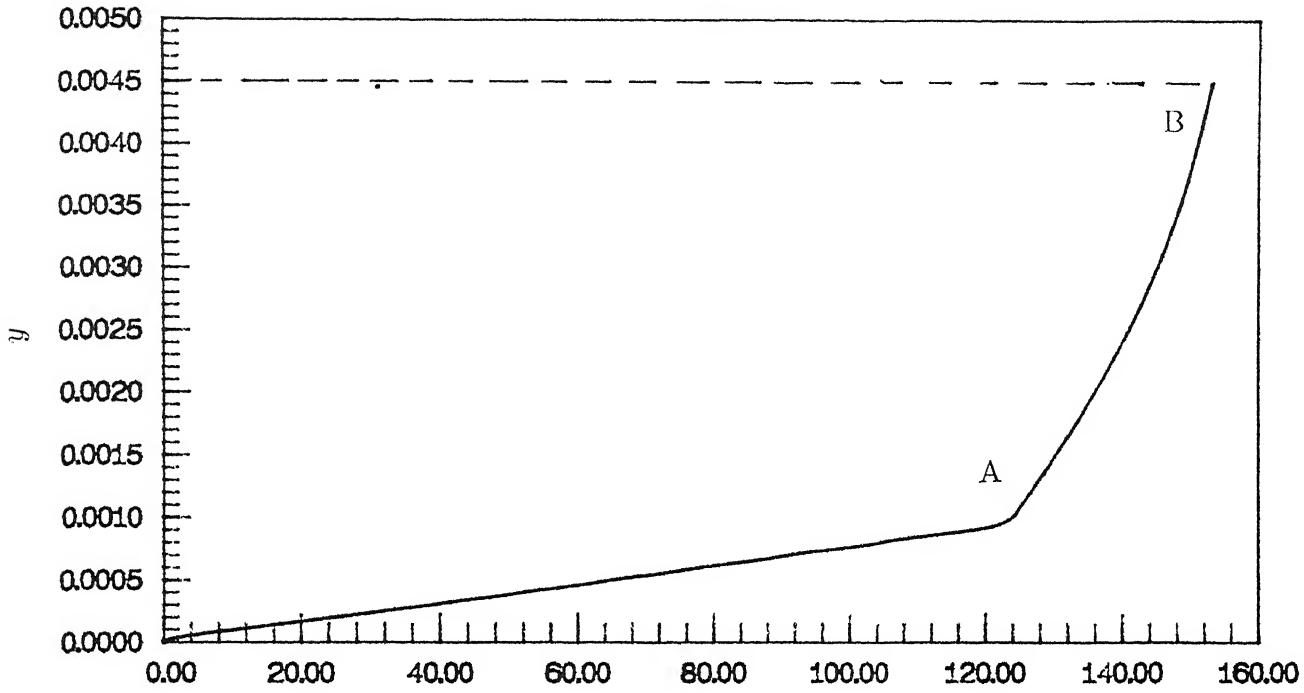

Figure 4.11: Turbulent Viscosity vs y at $Re_x = 5 \times 10^6$

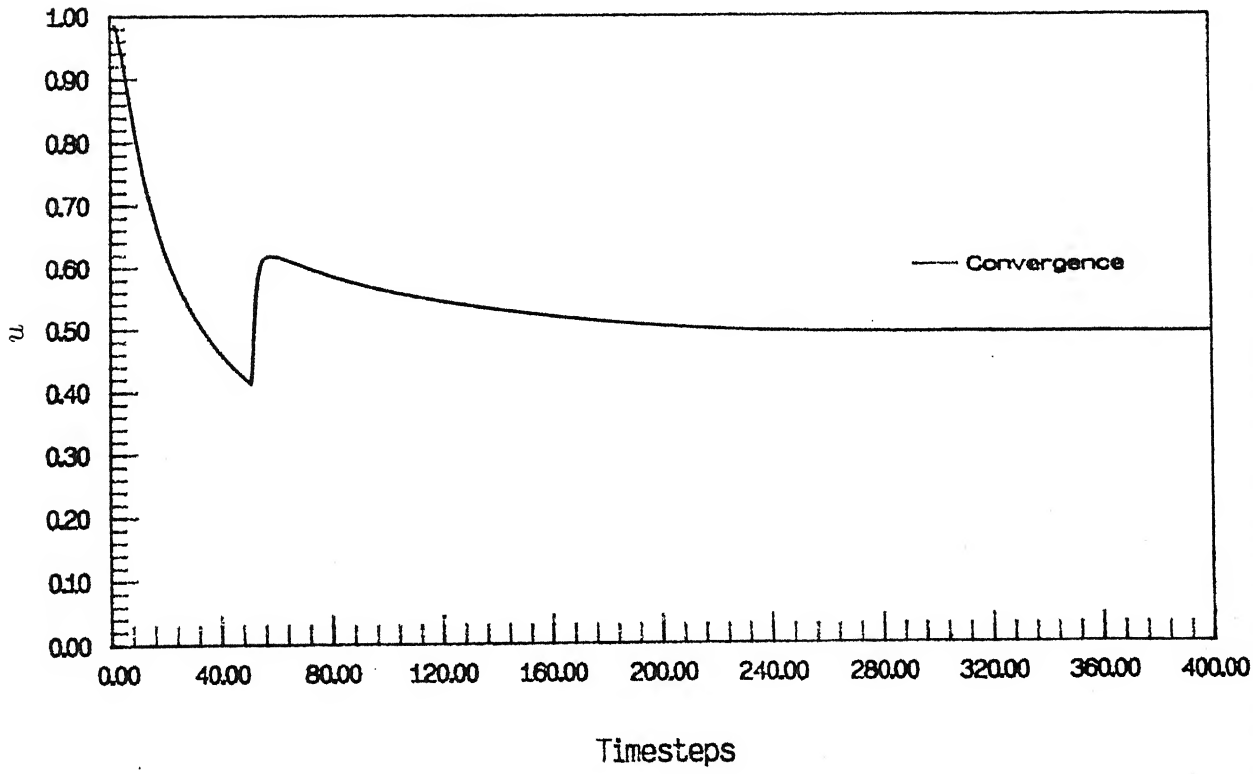

Figure 4.12: Convergence History of u at Grid Point (51,4) for Run 3

Chapter 5

Conclusions and Suggested Extensions

5.1 Conclusions

The time dependent, multi-dimensional, implicit finite difference scheme has been successfully applied to solve ensemble-averaged Navier-Stokes equations for a compressible, turbulent flow over a thin flat plate . The validity of the associated computer code has been established by comparing the code prediction with experimental/calculated results. A second order artificial viscosity model is used for the high Reynolds no. flows without much loss in accuracy in the solution to suppress the numerical oscillations. A fourth order dissipation term is used to smoothen the solution.

In the laminar region, the calculated velocity profile agreed with the well-known Blasius solution. For the turbulent flow, zero-equation Cebeci and Smith model is used and a reasonable agreement is found between the code predicted mean velocity u profile with the Simpson's experimental data. The calculated coefficient of local skin friction is compared with the known empirical correlation for it. Three computer runs are made for different input parameters and the results are plotted.

5.2 Suggested Extensions

The present numerical scheme and the associated computer code is capable of handling two-dimensional , non-reacting turbulent flow fields. It can be extended to deal with three-dimensional flows such as in rectangular intakes etc. including higher order turbulence models.

Another extension can be made with multicomponent , reacting flows which could be used, for instance, to solve the problem of the flat solid propellent grain burninig (Emmon's flat plate burning problem).

References

1. Anderson, D.A., Tannehill, J.C. and Pletcher, R.H. 1984. *Computational Fluid Mechanics and Heat Transfer.* Hemisphere Publishing Corporation, Washington.

2. Beam, R.M., Warming, R.F. *An Implicit Factored Scheme for the Compressible Navier-Stokes Equations.* AIAA. Journal.Vol.34. April, 1978. pp.393-402.

3. Bradshaw, P. 1976. *Turbulence.* Topics in Applied Physics. Springer-Verlag, Berlin.

4. Bradshaw, P., Cebeci, T. and Whitelaw, J. 1981. *Engineering Calculation Methods for Turbulent Flow.* Academic Press, New York.

5. Briley, W.R., McDonald, H. *Solution of Compressible Navier-Stokes Equations by Generalised Implicit Method.* Journal of Computational Physics. Vol.24. Aug., 1977. pp.372-397.

6. Briley, W.R., McDonald, H. *On the Structure and use of Linearised Block Implicit Schemes.* Journal of Computational Physics. Vol.34. Jan., 1980. pp.54-72.

7. Cannto, C., Hussaini, M.Y., Quarteroni, A. and Zang, J.A. 1987. *Spectral Methods in Fluid Dynamics,* Springer-Verlag, Berlin.

8. Cebeci, T. and Smith, A.M.O. 1974. *Analysis of Turbulent Boundary Layers.* Academic Press, New York.

9. Chen, K.K. and Thyson, N.A. *Extension of Emmon's Spot Theory to Flows on Blunt Bodies.* AIAA. Journal. No.5. 1971. pp.821

10. Deshpande, S.M. 1989 *Lecture Notes on Computational Fluid Dynamics.* National Aeronautical Laboratory, India.

11. Dhawan, S. and Narasimha, R. *Some Properties of Boundary Layer Flow during the Transition from Laminar to turbulent motion.* Journal of Fluid Mechanics, Vol.3. 1958. pp.418.

12. Douglas, J. and Gunn, J.E. *A General Formulation of Alternating-Direction Methods. Part-I, Parabolic and Hyperbolic Problems.* Numerische Mathematik, Vol.6, pp 428-453.

13. Emmons, H.W. *The Laminar, Turbulent Transion in a Boundary Layer, Part-1* Journal of Aeronautical Science, No.18. 1951. pp.490.

14. Fletcher, C.A.J. 1987. *Computational Techniques for Fluid Dynamics. vol. 1 & 2* Springer-Verlag, Berlin.

15. Hinge, J.O. 1959. *Turbulence, An Introduction to its Mechanism and Theory.* McGraw-Hill Book Company Inc., NewYork.

16. Lakshminarayana, B. *Turbulence Modelling for Complex Shear Flows.* AIAA. Journal, Vol.24, No.12. Dec. 1986. pp.1900-1917.

17. Landall, M.T. and Mollo-Christenson, E. 1992. *Turbulence and Random Process in Fluid Mechanics.* Cambridge University Press.

18. Roache. P.J. *On Artificial Viscosity.* Journal of Computational Physics, Vol.10, No.2. Oct., 1972.

19. Roache, P.J. 1985. *Computational Fluid Mechanics.* Hermosa Publishers, Albuquerque, New Mexico.

20. Roberts, G.O. *Computational Meshes for Boundary Layer Problems.* Proc. of 2nd Inter.Conf.on Numerical Methods in Fluid Dynamics. Springer-Verlag, Vol.8,1971.p 171-177.

21. Sabnis, J.S., Gibling.H.J., McDonald, H. *Navier-Stokes Analysis of Solid Propellent Rocket Motor Internal Flows.* Journal of Propulsion, Vol.5, No.6. Nov-Dec., 1989. pp.657-664.

22. Schlichting, H. 1968. *Boundary Layer Theory.* McGraw-Hill Book Company Inc., NewYork.

23. Shamroth, S.J., McDonald, H. and Briley, W.R. *Application of Navier-Stokes Analysis to Transonic Cascade Flow Fields.* ASME. paper. 82-GT-235, 1982.

24. Simpson, R.L. *Characteristics of Turbulent Boundary Layers at low Reynolds no. with and without Transpiration* Journal of Fluid Mechanics, Vol.42. 1970. pp.769-802.